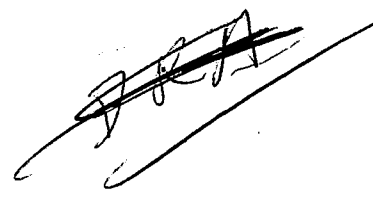SEPTEMBER 20, 1969 THROUGH JANUARY 29, 1971

CSL COORDINATED SCIENCE LABORATORY

FINAL
PROGRESS REPORT

JPL CONTRACT No. 952383

B. G. STREETMAN

(NASA-CR-126625)   A STUDY OF
IRRADIATION-INDUCED DEFECTS IN SILICON
USING LOW TEMPERATURE   B.G. Streetman
(Illinois Univ.)   May 1971   93 p   CSCL 10A

N72-24044

Unclas
G3/03   27900

UNIVERSITY OF ILLINOIS – URBANA, ILLINOIS

A STUDY OF IRRADIATION-INDUCED

DEFECTS IN SILICON USING LOW

TEMPERATURE PHOTOLUMINESCENCE

FINAL REPORT

Prepared for

Jet Propulsion Laboratory
California Institute of Technology

Under Contract JPL 952383

Principal Investigator

B. G. Streetman

May, 1971

Contributors to this report

B. G. Streetman

W. Dale Compton

Eric S. Johnson

Colin E. Jones

J. R. Noonan

E. S. Wong

TABLE OF CONTENTS

I. INTRODUCTION

In this report we describe the results of a research program investigating irradiation - induced defects in silicon, using low temperature photoluminescence as a probe of defect properties. The goal of this research was to gain new understanding of defects which degrade solar cell characteristics in a radiation environment. In this regard, an important aspect of this program was a study of radiation damage and annealing in lithium doped silicon, which is useful in reducing solar cell degradation.

Luminescence was used to study defects because this property reveals electron transitions through a number of defect energy levels at any given annealing stage; the luminescence spectra give excellent resolution of many defect energy levels; and these measurements can be used to give defect symmetry in the lattice, impurity dependence, and annealing properties.[1]

Many of the results reported here have been described previously by Spry,[1] Jones,[2] and Johnson.[3] In some cases where detailed discussion would detract from the readability of this report, reference is made to these earlier presentations. The report is divided into several sections. In Section II we describe the experimental approach to the luminescence measurements; in Section III we present data on spectra, stress effects, and annealing; in Section IV we analyze the results and describe our understanding of the nature of the defects; and in Section V we present a summary of results and recommendations.

II. EXPERIMENTAL PROCEDURE AND APPARATUS

2.1 General Description

The experiment consisted of irradiation of Si samples , measurements of low temperature photoluminescence with and without uniaxial stress, and annealing of irradiation damage. The luminescence measurements were performed in two systems, one using a 0.5 m Jarrell-Ash monochromator, and the other using a 0.75 m Spex monochromator. Figure 1 shows schematically the experimental arrangement for the Spex system; the essential features of the Jarrell-Ash system are similar. The sample was contained in a liquid helium cryostat with temperature control available by the rate of pumping of helium into the sample chamber. Electron-hole pairs were created by light in the visible spectrum which was focused on the sample. The infrared luminescence was collected and passed through the monochromator. The output of the monochromator was focused onto a cooled PbS detector, and the detector signal was processed using standard lock-in amplifier techniques. The luminescence spectrum was displayed on a chart recorder and in some cases simultaneously fed into an analog-to-digital converter which records the appropriate information on magnetic tape. This tape was then used in conjunction with a computer program to perform corrections for the system response.

Uniaxial stress was applied to the sample by differential thermal contraction mountings or by adjustable clamps. Irradiations were performed in a Van De Graaff accelerator with 0.5 to 3.0 MeV electrons. Annealing was performed in an oil bath or in a furnace, depending upon the temperature range. The defects studied were those which remain at room temperature
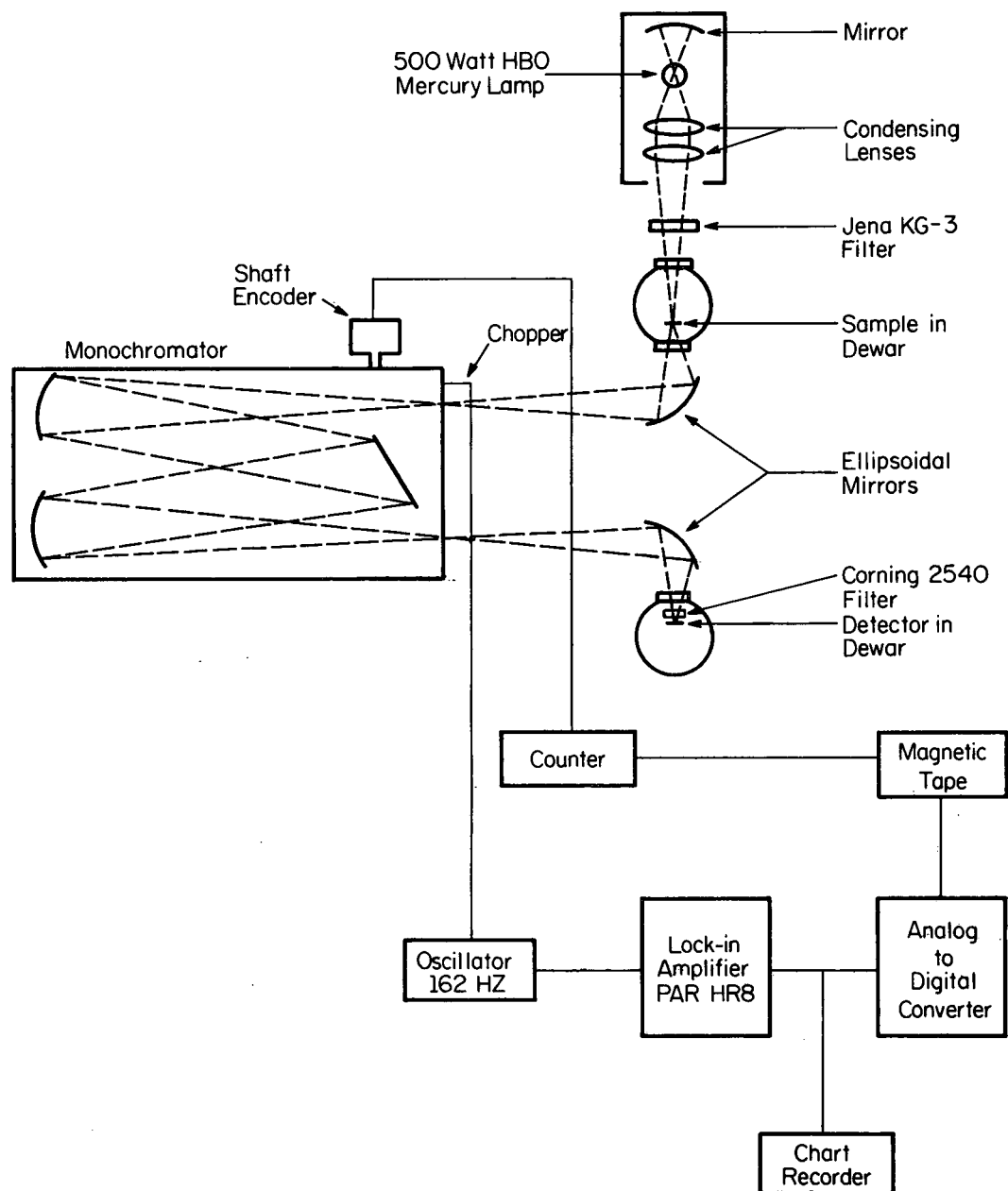
Figure 1. Schematic diagram of the Spex monochromator and apparatus.

and above. Irradiations were performed slightly below room temperature; the measurements of the luminescence spectra were made at low temperatures, typically 10° to $30^{\circ}K$; and annealing studies extended from room temperature to $600^{\circ}C$. Methods of investigation included study of line positions and their shape and temperature dependence, the effects of uniaxial stress on the position and splitting of lines, and the effects of thermal annealing.

2.2 Sample Preparation

2.2.1 Silicon Samples

All silicon used in the experiment came from single-crystal boules grown in the $\langle 111 \rangle$ direction, except for one $\langle 100 \rangle$ sample used in stress measurement. A description of the silicon used is summarized in Table 1. The oxygen concentration in pulled silicon is on the order of 10^2 times that of float zone silicon. Although luminescence has been seen in samples with a resistivity approaching 0.1 ohm-cm, samples in the resistivity range of 50 to 100 ohm-cm were used in these experiments. Consistently good luminescence intensity was obtained.

Table 1

Boule Designation	Method of Growth	Dopant	Room Temperature Resistivity (ohm-cm)	Manfacturer
T	Pulled	Phosphorus	100	Monsanto
1	Pulled	Phosphorus	102	NPC Metals & Chemicals
L	Float Zone	Phosphorus	70	Monsanto
2	Float Zone	Phosphorus	70	NPC Metals & Chemicals
P	Pulled	Boron	45	Monsanto
M	Float Zone	Boron	65	Monsanto
J	Pulled $\langle 100 \rangle$	Phosphorus	75	Semimetals

2.2.2 Cutting and Orientation

Rectangular samples used for broad band spectra measurements were cut to 2cm X 1cm X 1mm size from wafers sliced perpendicular to the boule axis. Stress samples were cut from oriented slices to close tolerances and had the following dimensions: length = 720 mils; width = 120 mils; thickness = 60 mils. All samples were lapped with #400 grit carborundum powder on a glass plate to remove saw marks. The stress samples were ground to a length between 716-715 mils. The other dimensions were not critical. Samples used in stress experiments were cut from boules and 2 and J. The crystallographic orientation of these samples was determined by Laue X-ray diffraction techniques.

2.2.3 Lithium Diffusion

Samples used in the study of the effects of diffused lithium were prepared as above and sent to outside laboratories for diffusion. Some samples, cut from Monsanto silicon, were lithium doped at the Goddard Space Flight Center, Greenbelt, Maryland. Other samples, cut from boule 2, were diffused by Centralab Semiconductor, El Monte, California. The concentration of electrically active lithium was determined by four-point probe resistivity measurements. Typically, the lithium concentration was between 10^{15} and 10^{18} atoms / cm^3. This concentration is much greater than the original doping of the silicon; thus the lithium interstitial donors dominated the conductivity.

2.2.4 Irradiation

The samples were irradiated with 3.0 MeV electrons from the University of Illinois Materials Research Laboratory Van de Graaff accelerator. Figure 2 shows a schematic of the irradiation sample holder attached to the accelerator beam port. The electron beam was defocused in the accelerator and further spread out in passing through the titanium beam-port window so that the irradiation was uniform over an area larger than the sample. Additional sheets of titanium were placed at the beam-port window to further diffuse the beam when several samples were simultaneously irradiated.

The beam current and total electron fluence were monitored with an aluminum Faraday cup of one square centimeter area and a thickness of 5/8 inch. The cup was mounted directly behind the sample and collected the current passing through the plane of the sample.

Temperature was measured by a copper-constantan thermocouple. The thermocouple and the sample were held against the sample holder with a phosphor-bronze wire spring. The sample was cooled by cold nitrogen gas directed into the sample holder. Sample temperature was $-10 \pm 10^{o}C$. Samples with no diffused lithium were irradiated to 10^{17} e/cm^2; lithium-diffused samples, to 10^{18} e/cm^2. Samples were turned over after accumulating half of the maximum fluence so that damage would be more uniform. All samples were immediately placed in dry ice ($-78^{o}C$) following accelerator shut down to prevent room temperature annealing.
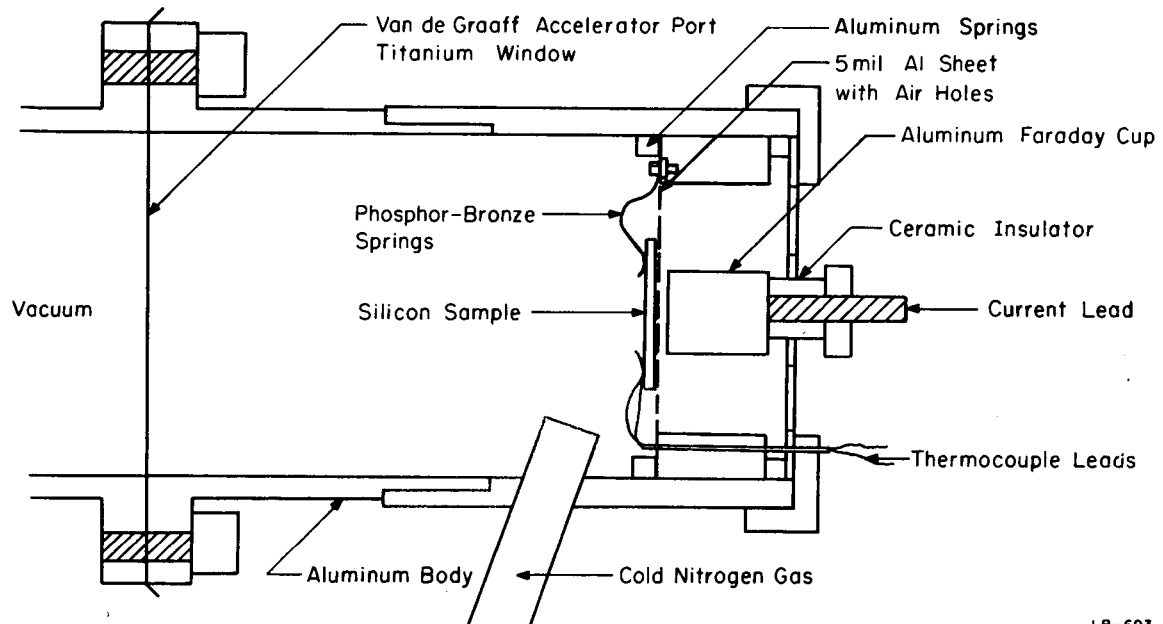
Figure 2. Schematic of the irradiation sample holder attached to the accelerator beam port.

2.2.5 Annealing

The sample was removed from storage in dry ice, etched, and placed in the dewar. The dewar was evacuated and cooled to liquid nitrogen temperature. This operation took about twenty minutes and is considered to be a room temperature anneal for that time period. An oil bath of Dow Corning 704 Fluid was used for annealing samples between room temperature and 300°C. The sample was placed in an aluminum bottle, sealed, and immersed in the oil. The anneal was rapidly quenched by removing the bottle from the bath and immersing it in Freon 11. The bath was heated to the approximate temperature by a flask heater and was maintained within $\pm 0.5^{\circ}$C. Temperature was measured by a chromel P-alumel thermocouple accurate to $\pm 0.5^{\circ}$C attached to the aluminum bottle. Samples annealed to less than 100°C were stored in dry ice to avoid room temperature annealing.

Anneals between 300°C and 700°C were performed in a tube furnace. Temperature was measured by a chromel P-alumel thermocouple built into the flat of a quartz spatula used to hold the samples. The oven temperature was simply controlled with a variac. This method of control resulted in a slow oven response to variac changes, but temperature fluctuations were limited to $\pm 1^{\circ}$C once stability was achieved. Upon completion of the anneal, samples were brought from maximum temperature to room temperature in thirty seconds. Samples used for broad spectra studies were annealed for twenty minutes. Samples used to obtain isochronal annealing curves were annealed for fifteen minutes.

2.2.6 Etching

Samples were etched prior to insertion in the dewar in order to produce a good optical surface and reduce nonradiative surface recombination. The etch was CP4A, $(5HNO_3, 3HF)$ made from Mallinckrodt Transistar grade chemicals. The etch was quenched by flushing with a large quantity of distilled water. The critical dimensions of stress samples were protected from etch by painting them with Unichrome Stop Off Lacquer (323 red lacquer) thinned with acetone. The lacquer was easily peeled from the samples after etch. Samples were dried on filter paper and placed in the dewar. The dewar was quickly evacuated to minimize the formation of oxide on the sample.

2.2.7 Mounting

The samples which were measured with no stress applied were held in place in the cryostat with a phosphor bronze spring. This spring also held a thermocouple to the sample. The samples used in the stress measurements were mounted in two ways. The first was to hold the sample against the sample holder using the phosphor bronze spring and apply stress using adjustable clamps (Fig. 3). In the second method the crystal was placed in a slot cut in a piece of brass. The slot was milled out so that its length was 720 mils. This is the same length as the samples and they fit tightly in this dimension. The thermal contraction $\Delta \ell/\ell$ of brass is 4×10^{-3} over the range $300^{\circ}K$, whereas for silicon it is 2.6×10^{-3} for the same temperature range. When the sample in this brass holder is cooled in the cryostat, the brass contracts upon the silicon and provides a uniaxial compression along the length of the crystal.

Helium Chamber

Needle valve

Copper Tube with
Heater Wire

Light Pipe

Sample Area

Movable Clamp

Gear Drive
for Clamp
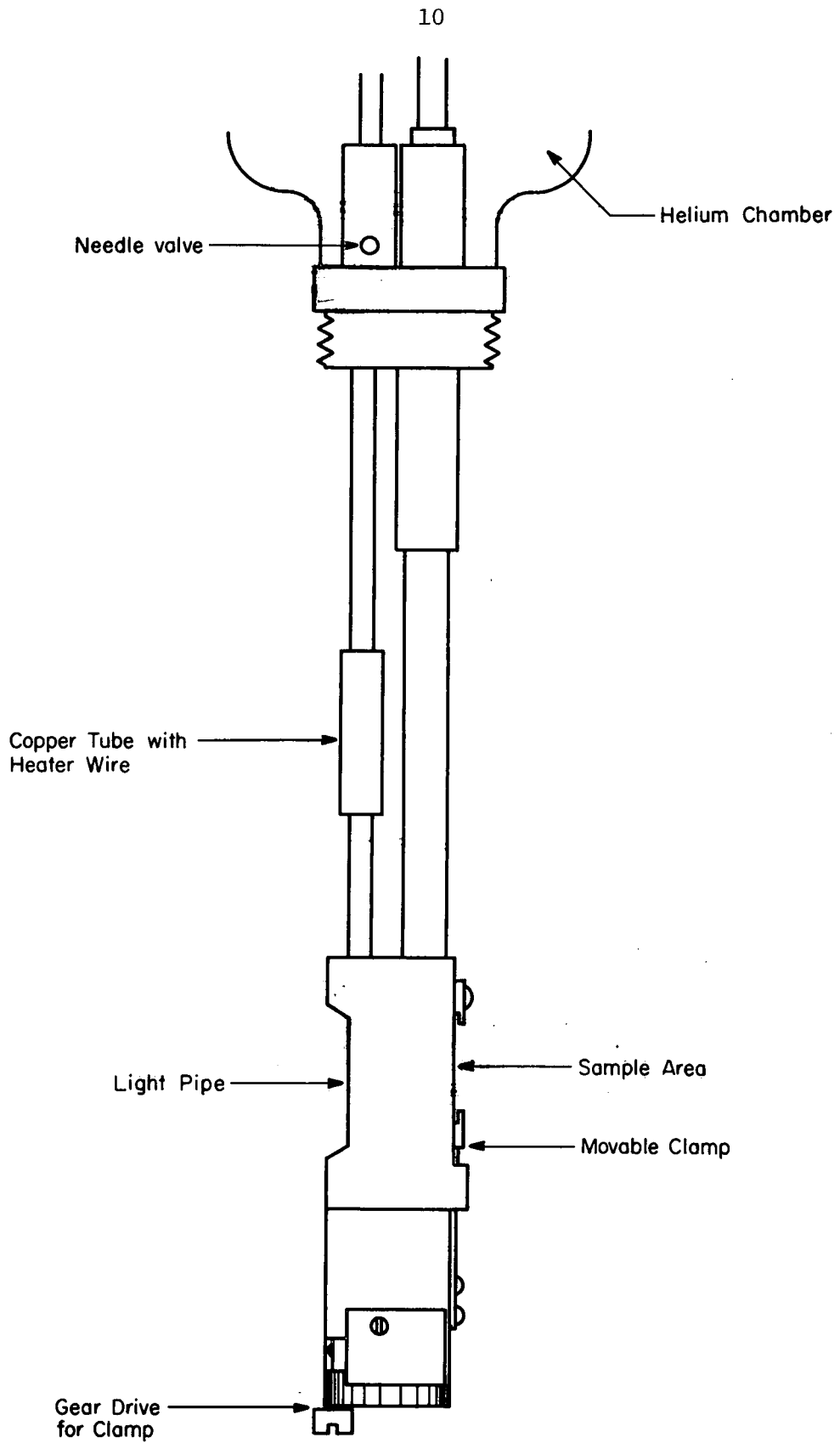
LR-407

Figure 3. Helium dewar sample holder with the variable stress clamps.

2.3 Optical Detection

The detector used in this investigation was a Hughes Santa

Barbara Research Center PbS detector with a maximum defectivity D* of

$4.3 \cdot 10^{11} \frac{cm(H_z)^{\frac{1}{2}}}{watt}$. The detector was operated at $-78^\circ C$ and was shielded

by a copper cold-shield and a cooled Corning #2540 color filter on which

the radiation from the monochromator impinged.

The windows, filters, grating, and atmosphere in the optical

path have wavelength dependent transmission properties. The detector

response is also wavelength dependent. Correction factors were calculated

from data obtained using a blackbody source in place of the sample.

The ratio of the observed signal to the calculated number of

photons from the blackbody was computed for each wavelength over the

range of wavelengths of interest. The point having the largest ratio

was taken as a point for a correction factor of one. The correction

factor needed to bring each of the other ratios up to this value was

calculated and plotted as a function of photon energy. Monochromator

wavelength calibration and resolution over the wavelength range 1.05 to

1.70 μ were determined using a low-pressure mercury lamp.

Measurements with the Spex monochromator reported in this inves-

tigation were made with a 1200 ℓ/mm Bausch & Lomb Replica grating.

Polarization correction factors were also obtained using the

blackbody source and a type HR infrared polaroid placed in the optical

path. The component perpendicular to the stress direction was 3.18 times

more intense than the parallel component. General corrections for

grating polarization were obtained by multiplying the parallel component

by 3.18. The polarization correction factor was constant over the wavelength interval 1.180 to 1.195 μ, in which stress-split spectra were observed.

2.4 Data Analysis

The data analysis for luminescence spectra was basically the same for both monochromator systems. Raw data showing the relative luminescent intensity as a function of wavelength were recorded on chart paper. Corrections for wavelength, system response, and normalization were applied to the data, which was plotted in final form as relative photon intensity per wavelength interval versus photon energy. These corrections were made by hand or using the computer program described above.

The isochronal annealing curve of a luminescence peak was determined by comparing the intensity of the luminescence peak after various anneals with the intensity before anneal. For each observation the sample was annealed, etched, and inserted in the dewar. The cold dewar was then placed in the monochromator system. The detector dewar was also removed from the system, evacuated, cooled, and replaced for each run.

Changes in the luminescence intensity can result from each of these procedures. Variation in sample luminescence intensity can also be caused by variations in sample observation temperature and irregularities in surface treatment. Nevertheless, corrections for these variations and for the apparatus were determined and applied to the data.

Variations in the monochromator system's sensitivity were accounted for by measuring the signal from the mercury lamp under set conditions with the sample dewar removed. This measurement accounted for variations in line voltage to the mercury lamp and the system electronics, the detector alignment, and the tuning of the lock-in amplifier. The sample dewar position in the system was duplicated exactly. A correction for amplifier gain scale setting was also applied. Corrections for variation in sample observation temperature were made from a plot of intensity as a function of observation temperature.

III. EXPERIMENTAL DATA

Data taken during the course of this research will be presented in this section. These data consist of luminescence spectra from irradiated silicon which had been annealed both at room temperature and at higher temperatures. Isochronal and isothermal annealing of certain luminescence lines is also shown. Results for silicon without lithium doping will be presented first, followed by data on lithium-diffused silicon. The data on lithium-diffused silicon consist of luminescence spectra, in addition to the results of extensive measurements on the properties of the major lithium-dependent center.

3.1. Silicon Without Lithium Doping

Figure 4 shows the intrinsic luminescence spectrum observed from unirradiated 100 ohm-cm n-type pulled silicon. Similar spectra were seen in samples from the other boules listed in Table 1. This spectrum is in excellent agreement with that observed by Haynes, which was attributed to free exciton recombination.[4]

After irradiation the intrinsic luminescence of Figure 4 is no longer seen. Instead several lower energy peaks are seen between about 0.5 eV and 1 eV. A typical spectrum observed after irradiation is shown in Figure 5. Several sharp peaks can be easily distinguished in Figure 5; these have been labeled with the letters A through G. As discussed below, the half-widths of these lines are less than kT and are not thermally broadened. Since these peaks do not exhibit phonon participation, they will be referred to as zero-phonon lines.
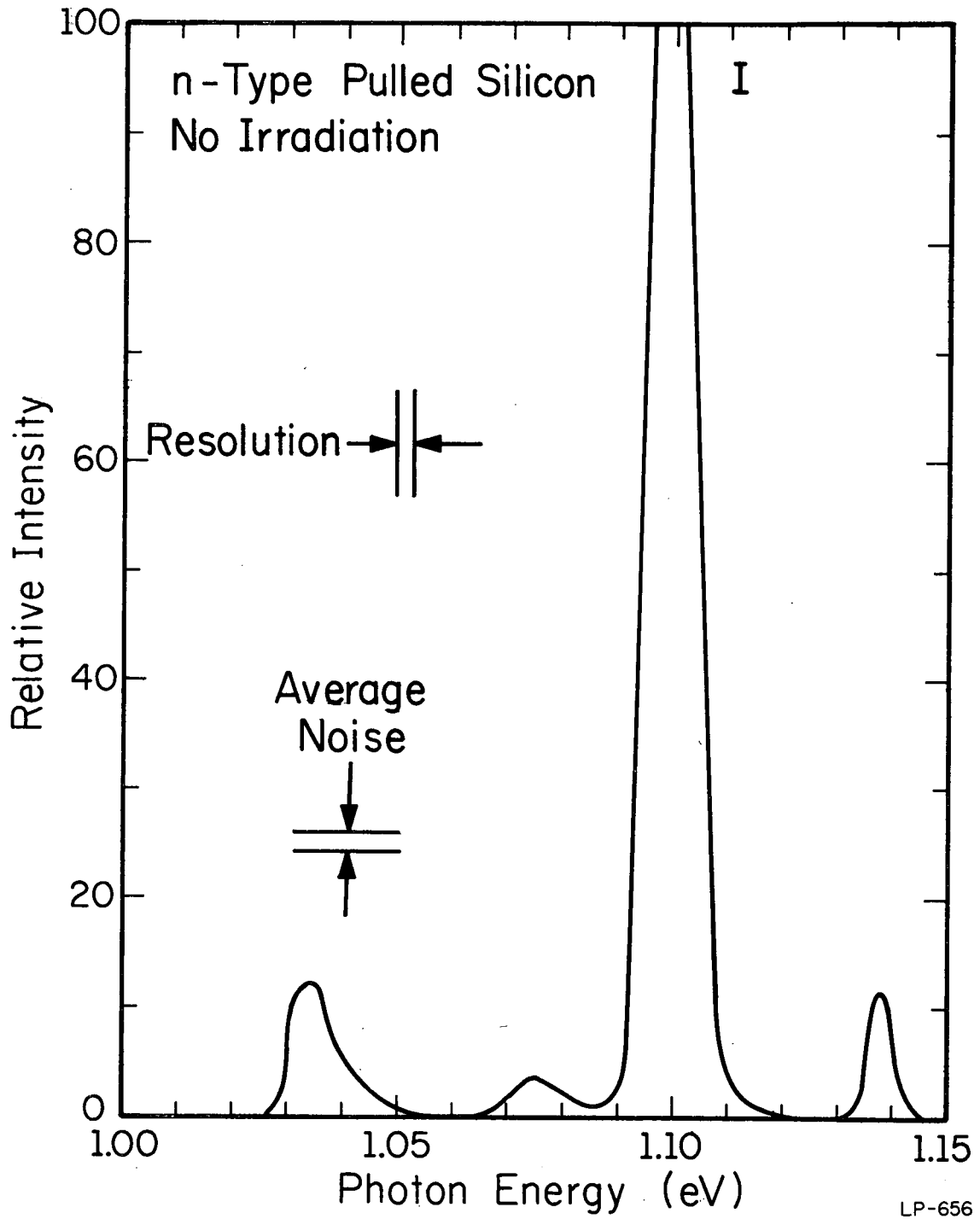
Figure 4. Recombination luminescence from unirradiated 100 ohm-cm phosphrous doped ($<10^{14}$atoms/cm^3), pulled silicon. The spectrum was observed at 13°K.
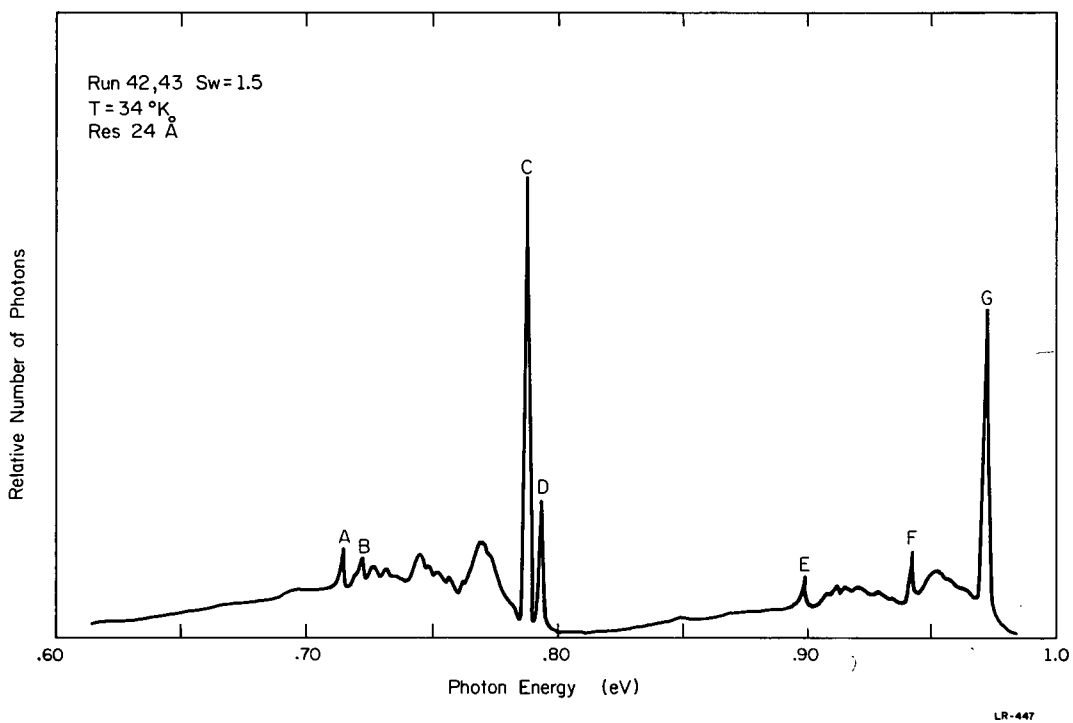
Figure 5. Recombination luminescence from n-type pulled silicon at 34°K. The sample was irradiated at room temperature with 2.5 MeV electrons to a fluence of 10^{17}e/cm^2.

There are two main spectral groups which always seem to appear as units. Peaks A, B, and C and most of the broad peaks in between have been observed in the same intensity ratios in all samples measured. Peak D is seen with this group but its intensity varies exponentially with temperature with respect to the intensity of peak C. Peaks E and G and most of the broad peaks in between them form the second group and have always been seen in the same proportions. Peak F has been seen in only a few samples.

The luminescence observed from irradiated silicon depends critically on the fluence to which the sample has been exposed. Intrinsic luminescence was observed for fluence levels below a "threshold"; the intrinsic luminescence vanished and luminescence involving deep recombination levels appeared for a fluence above the threshold. At the threshold fluence, intrinsic luminescence and defect luminescence have similar intensities. The observed thresholds for boules L, M, T, and P are given in Table II.

Table II

Material	Boule	Threshold (3 MeV electrons/cm^2)
n-type float zone	L	$\sim 10^{16}$
p-type float zone	M	$< 10^{17}$
n-type pulled	T	$\sim 10^{14}$
p-type pulled	P	between 10^{16} and 10^{17}

In general, the increase in defect luminescence intensity produced by increased irradiation fluence was not linearly proportional to the fluence, the proportionality vary for samples from different boules. Irradiation

to high fluence ($\gtrsim 10^{18}$ e/cm^2) generally reduced the intensity from the maximum which was obtained for fluences of $\sim 10^{17}$ e/cm^2.

3.1.1. The 0.79 eV and 0.97 eV Spectra

The strong lines C at 0.79 eV and G at 0.97 eV in Figure 4 were intense enough to be measured over a fairly broad range of temperature and at various resolutions. The intensity of the 0.79 eV C line peaks at $\sim 25^{\circ}$K and decreases approximately exponentially at both lower and higher temperatures. The slope corresponds to 20 meV ± 5 meV on the high temperature side and to -6 meV ± 1 meV on the low temperature side.

The halfwidths of the 0.79 eV and 0.97 eV lines as a function of temperature are shown in Figure 6. A log-log plot of the broadening vs. temperature can be fit by a straight line with a slope of 3.3 ± .3 for the 0.79 eV peak. Thus, the broadening goes approximately as $T^{3.3}$. A similar plot of the shift in peak position versus temperature shows that the shift is proportional to $T^{2.4}$.

Similar results were obtained for the G peak at 0.97 eV. For this line the intensity peaks at about 35°K. The high energy slope is 35 meV ± 5 meV and the low temperature slope is -3.5 meV ± 1 meV. The halfwidth of the line goes approximately as $T^{4 \pm .7}$. The shift in peak position goes approximately as $T^{2.4}$.

3.1.2. Other Peaks

The other lines A, B, D, E, and F in Figure 5 all seemed to be as sharp as the lines C and G when they were measured with the same resolution. Their intensities were smaller and therefore the resolution
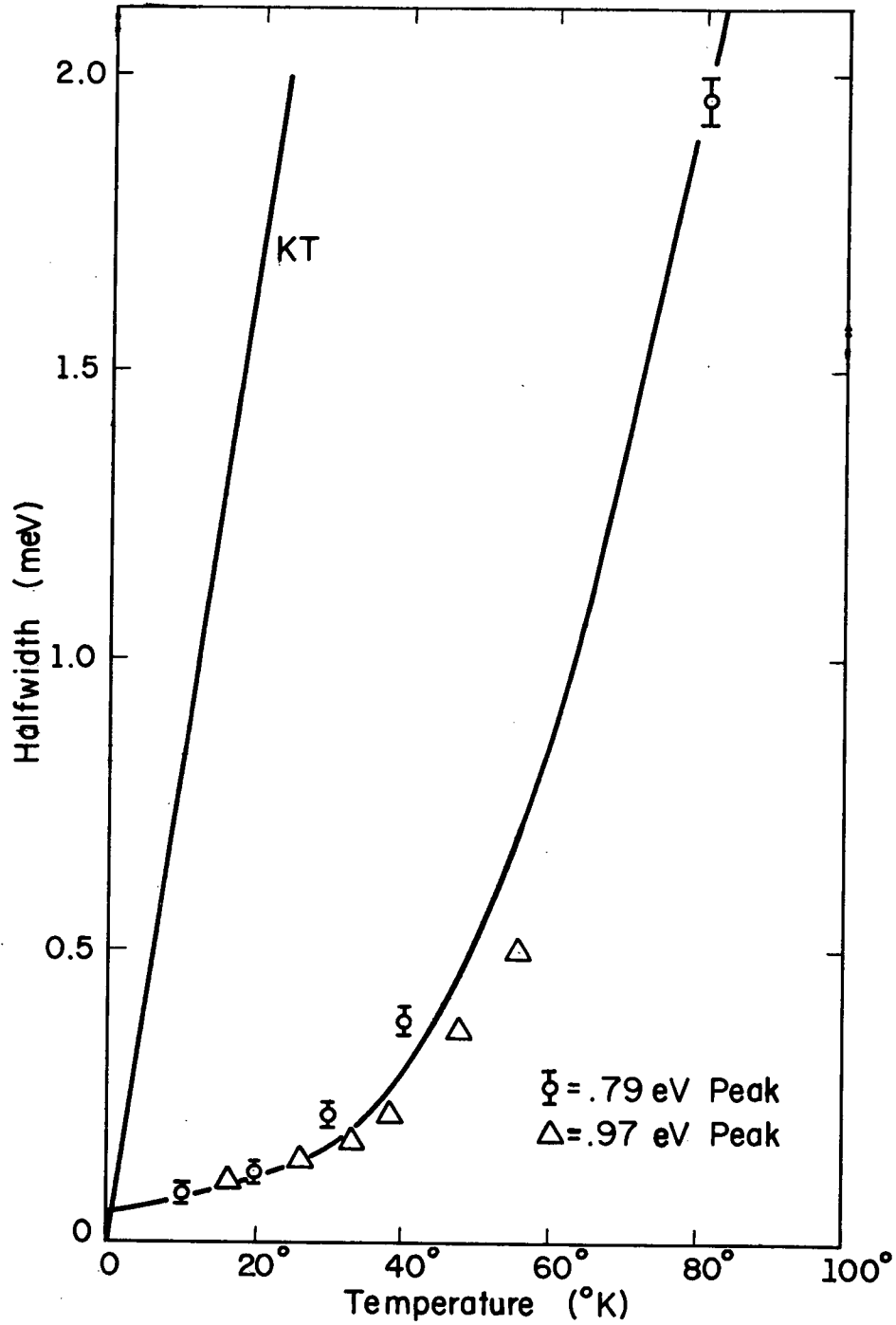
Figure 6. The half-widths of the zero-phonon peaks at 0.79 eV and
0.97 eV as a function of temperature. A plot of the
function kT has been included (for reference).

used to measure them was limited to above 0.4 meV. The intensities of
these peaks all go through a maximum as temperature is varied. The temperature
dependence of these smaller peaks is shown compared to that of strong lines
C and G in Figure 7. The data were taken from one sample during one data
taking session. Peaks A, B, and C all have the same temperature dependence.
Peak D varies exponentially with respect to peak C with an activation energy
of 4.0 meV ± 1 meV. The separation of lines C and D as measured optically
is 5.6 meV. The intensities of peaks C and G are not related in any simple
exponential way.

The integrated intensity of the sharp line C at 0.79 eV is approxi-
mately 1/10 that of the total group from 0.8 eV to 0.5 eV when measured with
a 24 $\overset{o}{A}$ resolution. This ratio was independent of temperature over the range
examined which was 10°K to 45°K. The same property was examined by looking
at the ratio of the intensity of the C peak to that of the first broad peak
at 0.76 eV. Again this ratio was constant over the temperature range
measured. Peak G at 0.97 eV gave the same results.

3.2. Annealing Data

3.2.1. n-Type Float Zone Silicon

Figures 8 and 9 show the luminescence spectra from irradiated
n-type float zone silicon after successive twenty-minute anneals in the
temperature range 23 to 600°C. The spectrum observed after room temperature
anneal (bottom Fig. 8) was identical to the spectrum associated with the
0.97 eV zero-phonon line (Fig. 5), with the exception of a tail extending
to higher energy which has a definite point of inflection. This high-
energy tail is referred to subsequently as the "pretail". The pretail
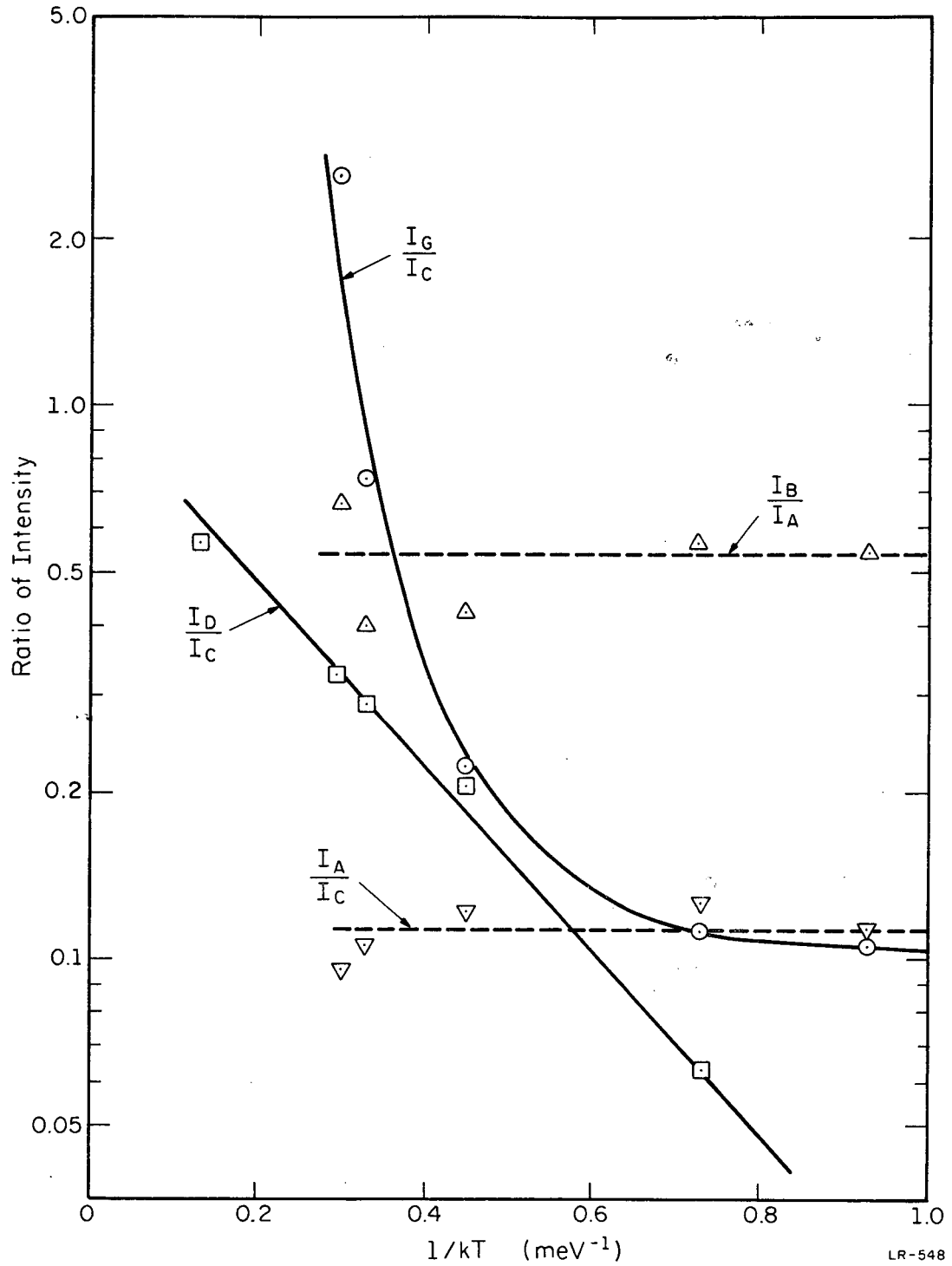
Figure 7. The ratios of several peak intensities versus 1/kT.

⊙ I_G/I_C

▫ I_D/I_C

△ I_B/I_A

▽ I_B/I_A
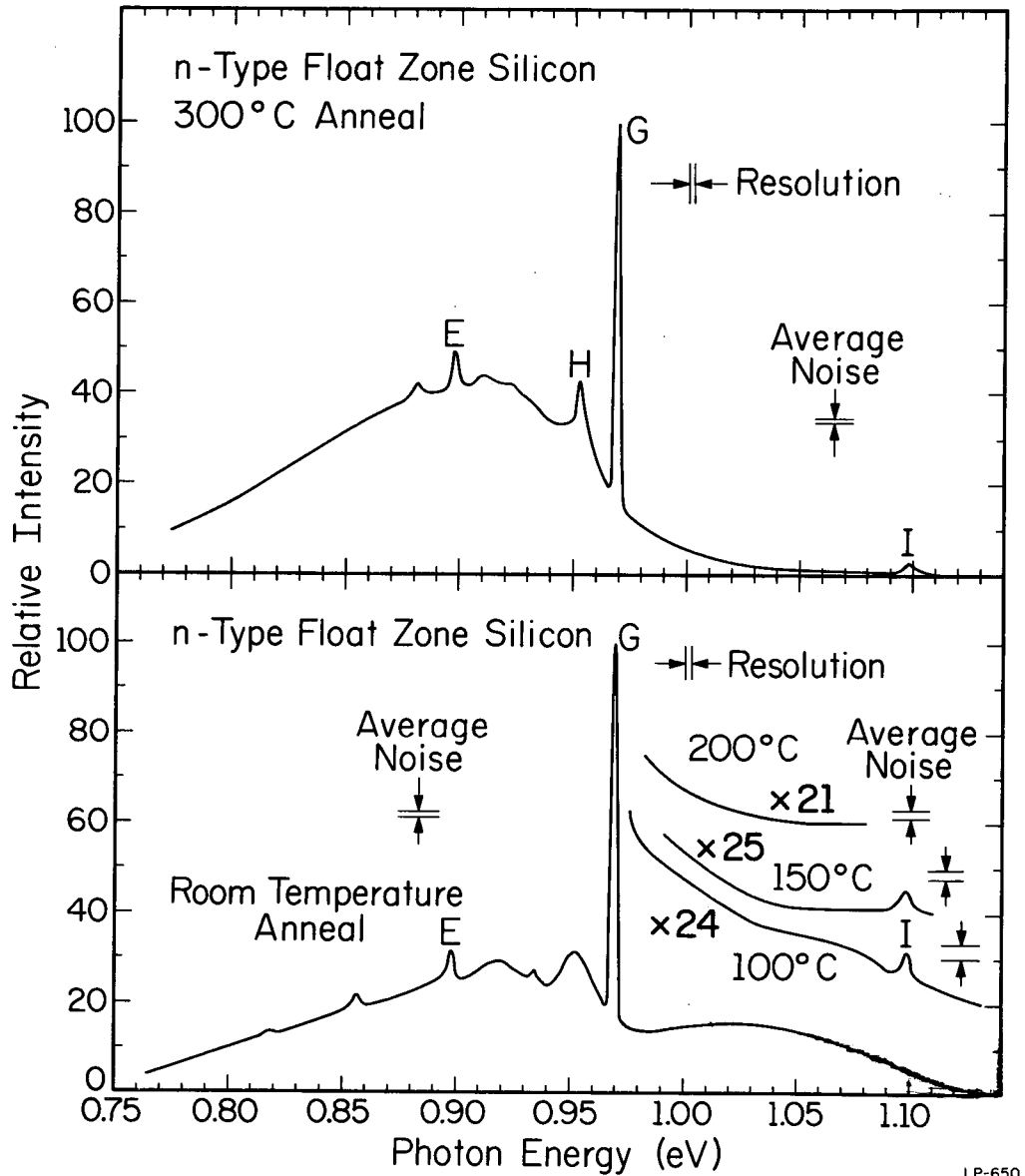
Figure 8. Luminescence spectra from n-type float zone silicon irradiated to a fluence of 10^{17} e/cm^2. Full spectra for twenty-minute anneals at room temperature (23°C) and 300°C are shown. Partial spectra at high gain for successive anneals at 100, 150, and 200°C are also shown. These curves have been translated vertically for clarity. The spectra was observed near liquid helium temperature.

Figure 9. Luminescence spectra from n-type float zone silicon irradiated to a fluence of 10^{17} e/cm^2. The sample was previously annealed in the range 23 to 30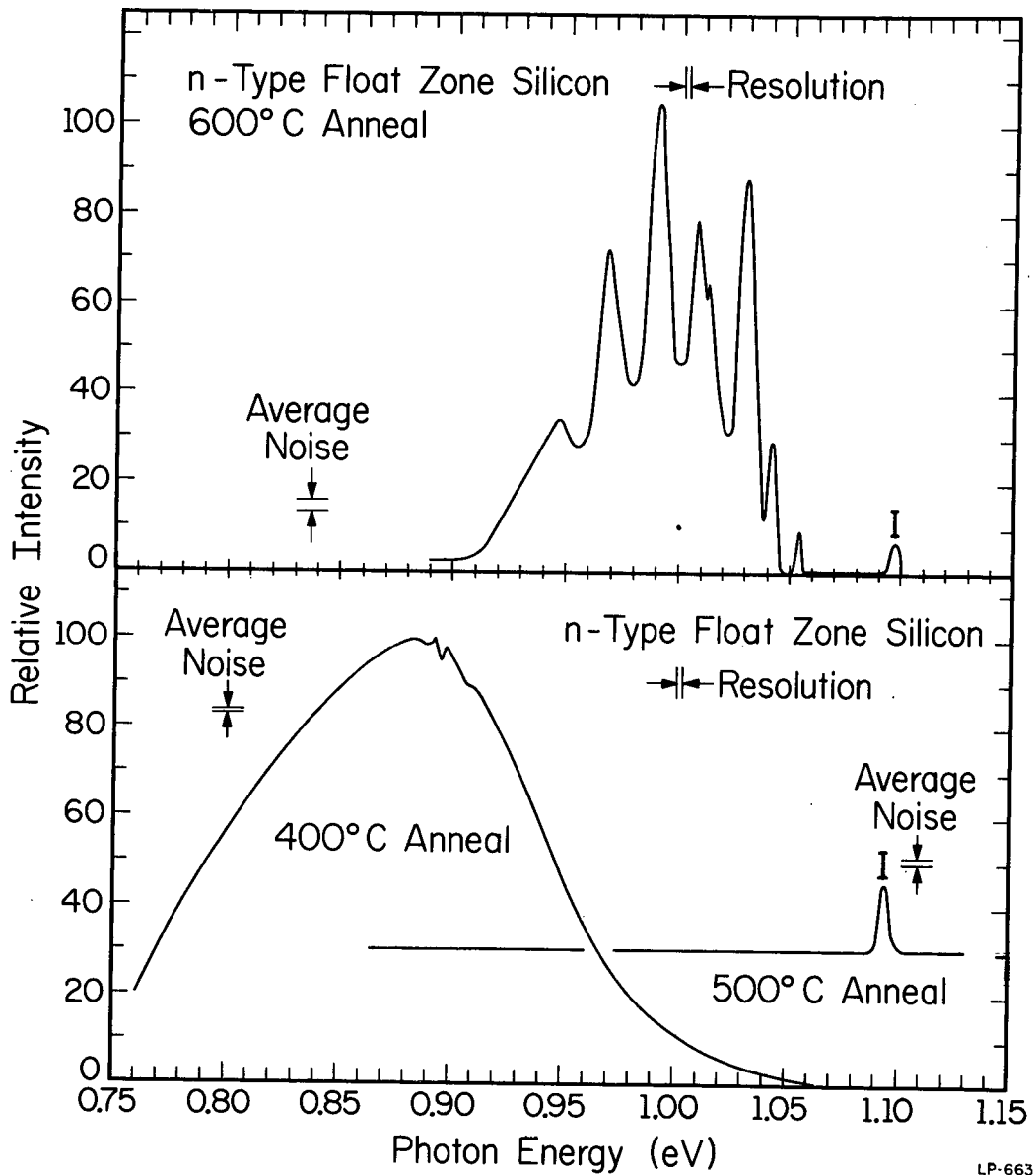0°C. (See Fig. 8). The spectra shown here were obtained after additional twenty-minute anneals at 400, 500, and 600°C. The spectra were observed near liquid helium temperature.

vanished after anneal at 100°C. Figure 8 also shows the appearance and disappearance of the intrinsic luminescence peak I, in the temperature range 23 to 300°C.

Zero-phonon line H (0.953 eV) is shown in the 300°C anneal spectrum (top Fig. 8). This weak peak is independent of the 0.97 eV spectrum; it appeared following anneal at 275°C and vanished after anneal at 350°C. Figure 9 shows the spectrum following 400°C anneal. The 0.97 eV spectrum has vanished, leaving a broad band with no prominent structure. This broad band vanished following 500°C anneal, leaving only intrinsic luminescence peak I. A new spectrum consisting of a series of sharp lines appeared following 600°C anneal (top Fig. 9).

The center associated with the zero-phonon line at 0.97 eV was the only strong luminescent center observed in irradiated n-type float zone silicon for samples annealed in the temperature range 23 to 600°C. The isochronal annealing of the 0.97 eV zero-phonon line is shown in Fig. 10. The curve drawn is the best fit consistent with the uncertainty limits of the data. The intensity of this peak increased by a factor ∿30 between 23°C and 100°C. The peak began to anneal out at 200°C, had half-maximum intensity at 280°C, and vanished following 325°C anneal.

3.2.2. p-Type Float Zone Silicon

Figures 11 and 12 show the luminescence spectra observed for irradiated p-type float zone silicon after successive anneals in the temperature range 32 to 700°C. The spectrum seen after a twenty-minute room temperature anneal (bottom Fig. 11) had an unusually intense

n-Type Float Zone Silicon

15 Minute Isochronal Anneal
0.97 eV Zero Phonon Line

LS-669
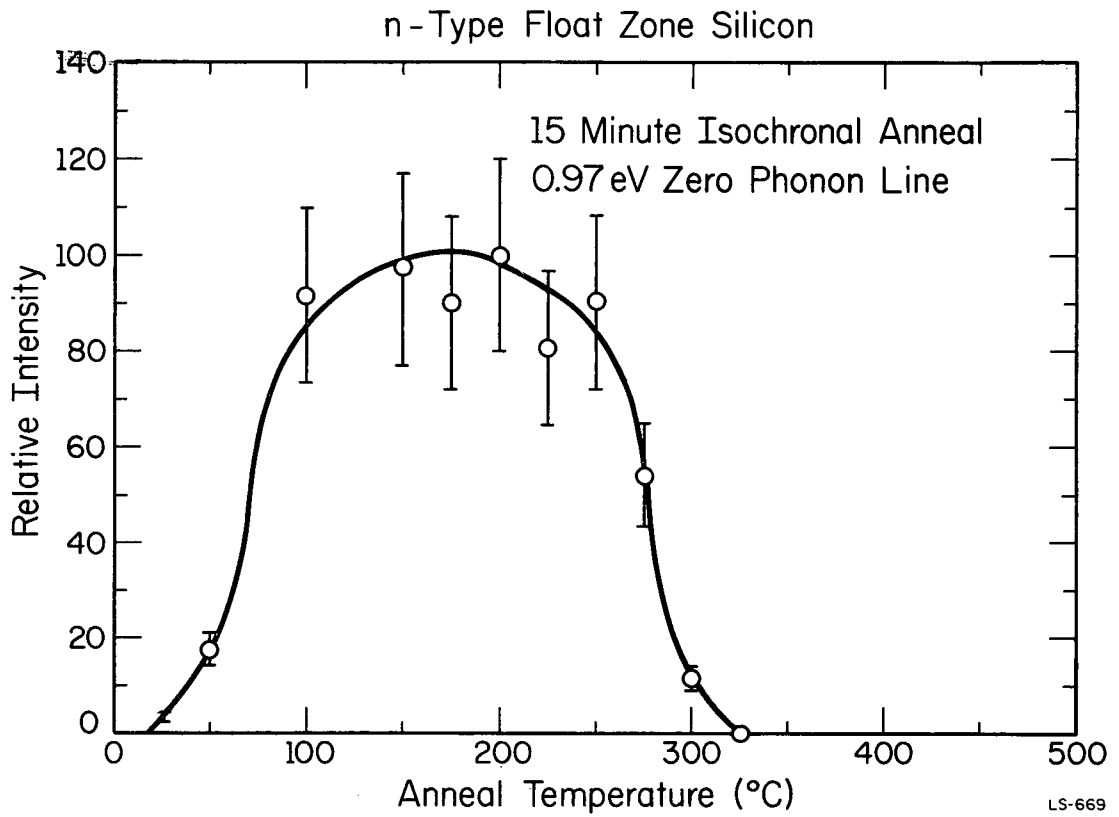
Figure 10. The isochronal annealing of zero-phonon peak G (0.97 eV)
in n-type float zone silicon.
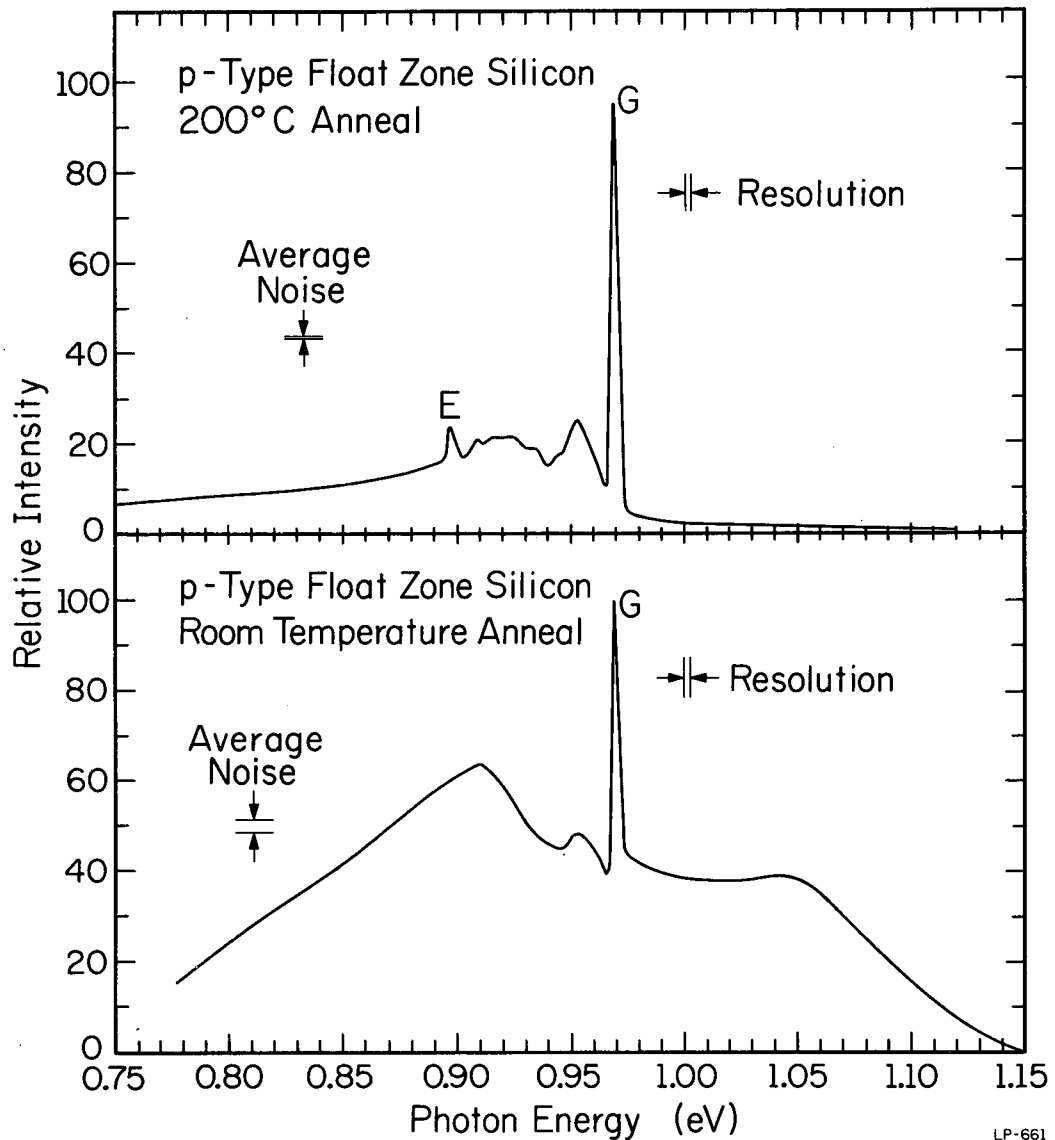
Figure 11.   Luminescence spectra from p-type float zone silicon
irradiated to a fluence of 10^{17} e/cm^2. Spectra
observed after twenty-minute room temperature (23°C)
and 200°C anneals are shown. The spectra were observed
near liquid helium temperature.
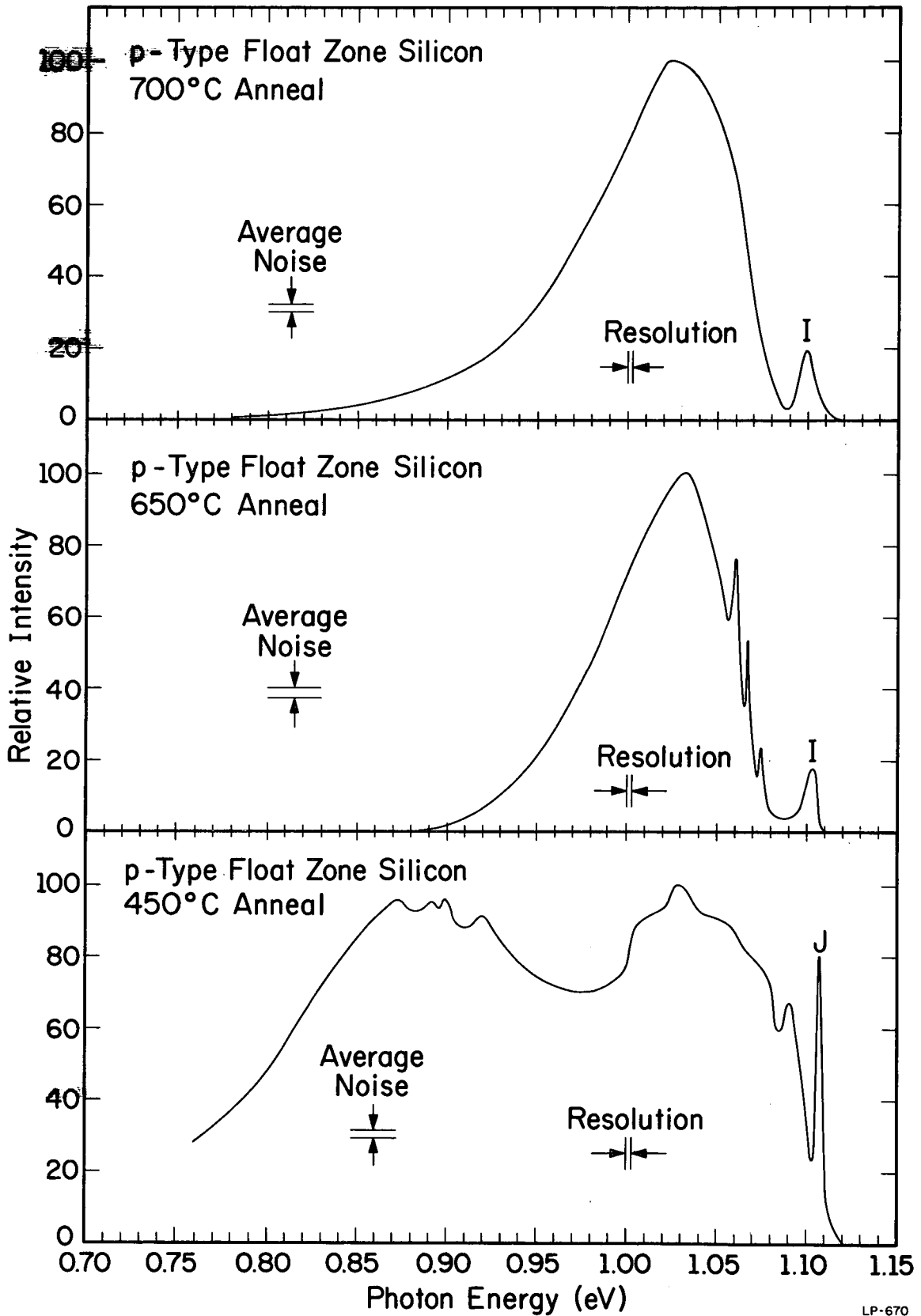
Figure 12. Luminescence spectra from p-type float zone silicon irradiated to a fluence of 10^{17} e/cm^2. The sample was previously annealed in the temperature range 23 to 400°C (Fig. 11). The spectra shown here were obtained after additional twenty-minute anneals at 450, 650, and 700°C. The spectra were observed near liquid helium temperature.

luminescence at energies greater than 0.97 eV (pretail), and as a consequence,
displays only slight resemblance to the spectrum of the 0.97 eV defect shown
in Fig. 5. Only peak G and its TA phonon replication can be distinguished.
The pretail annealed out near 200°C, leaving a spectrum (top Fig. 11)
identical to that of the 0.97 eV defect. Peak G annealed out by 300°C.

Figure 12 (bottom) shows a new spectrum that grew in between 300°C
and 450°C. The most significant feature of this spectrum was the structure
in the energy interval 1.00 to 1.12 eV, dominated by zero-phonon peak J
(1.108 eV). Other structure appearing in this spectrum at photon energies
between 0.95 eV and 0.80 eV was similar to the spectrum of irradiated n-type
float zone silicon at these anneal temperatures (bottom Fig. 9). Peak J
was observed in the spectra from two of the three samples cut from boule M,
and from a single sample of DuPont p-type float zone silicon. In the single
case where this spectrum was not seen, the 400°C anneal spectrum in the
bottom of Fig. 9 was seen instead. Zero-phonon peak H was also seen in
this atypical sample.

All luminescence was quenched by a 500°C anneal. At higher anneal
temperatures (600 to 700°C), two different weak spectra were seen in p-type
float zone silicon. In the first case, the spectrum shown in the middle
of Fig. 12 was seen, and in the second case a spectrum identical to the
top spectrum in Fig. 9 was observed. Further anneal produced the spectrum
shown at the top of Fig. 12. The float zone samples used in this investiga-
tion were examined by a hot-point probe to determine the type of majority

carrier. The sample designations were found to be correct; therefore, the variety of spectra could not be explained in terms of mistaken sample designation.

Figure 13 shows the isochronal annealing of strong zero-phonon lines G at 0.97 eV and J at 1.108 eV found in p-type float zone silicon. The annealing curve drawn for peak G is the best fit consistent with the uncertainty limits of the data. The intensity of peak G increased by a factor of ∿30 between anneals at 32°C and 150°C. The peak began to anneal out near 200°C, reached half-maximum near 250°C, and vanished by 300°C. Peak J was first observed at 300°C. It reached its maximum intensity at 450°C and vanished at 500°C.

3.2.3. n-Type Pulled Silicon

Figures 14, 15, and 16 show the luminescence spectra from n-type pulled silicon after successive anneals in the temperature range from 32 to 600°C. The room temperature anneal spectrum shown in the bottom of Fig. 14 is consistent with the spectra shown in Fig. 5. In addition, a weak pretail was observed in this spectrum at very high gain. The form of the pretail usually resembled those observed in spectra from float zone silicon. On two occasions, however, the structure shown in the bottom of Fig. 14 was seen; the pretail vanished following anneal at 50°C. Peak G began to anneal out at 200°C and vanished at 275°C.

Three new zero-phonon peaks were observed following 400°C anneal. These are designated as F (0.950 eV), K (0.925 eV), and L (0.767 eV) in the bottom of Fig. 15. Further anneal to 450°C reduced the intensity of peaks C and F (top Fig. 15). Peaks K and L were observed through the
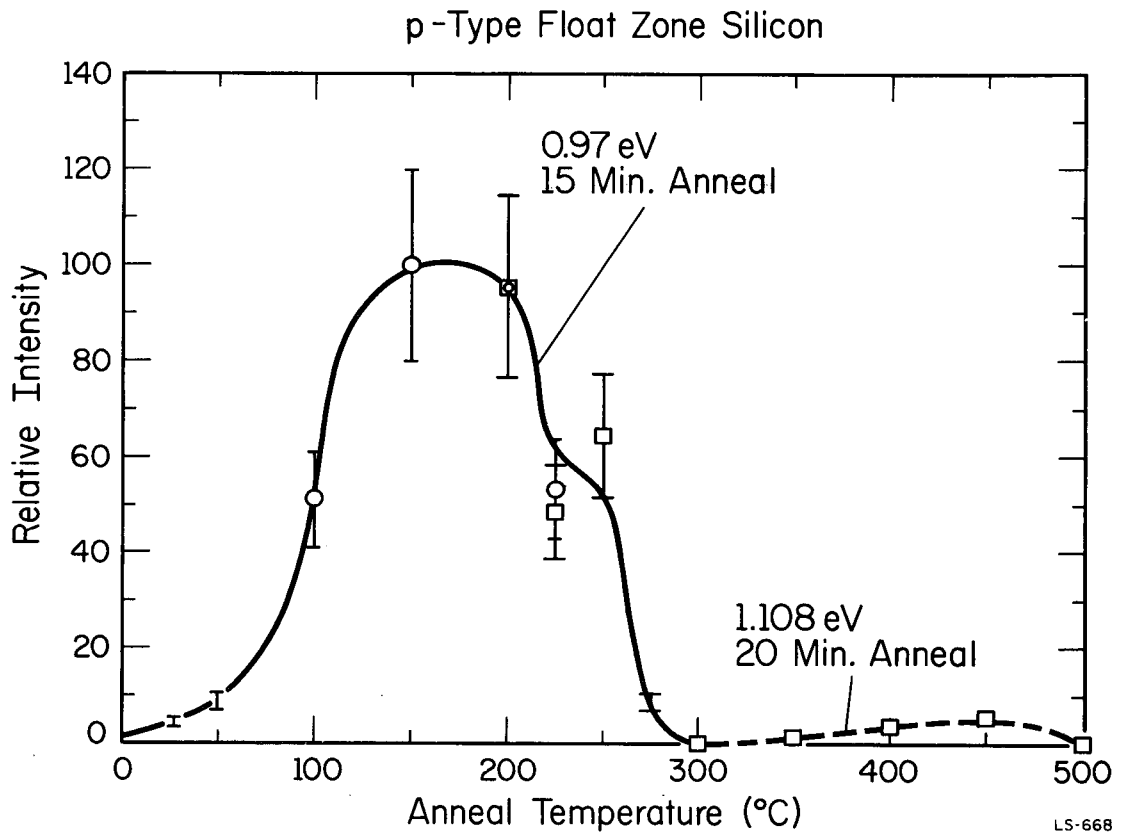
Figure 13. The isochronal annealing of zero-phonon peaks G (0.97 eV), and J (1.108 eV), in p-type float zone silicon. Two samples were used: ○ ..... Sample No. 64; □ .... Sample No. 43.
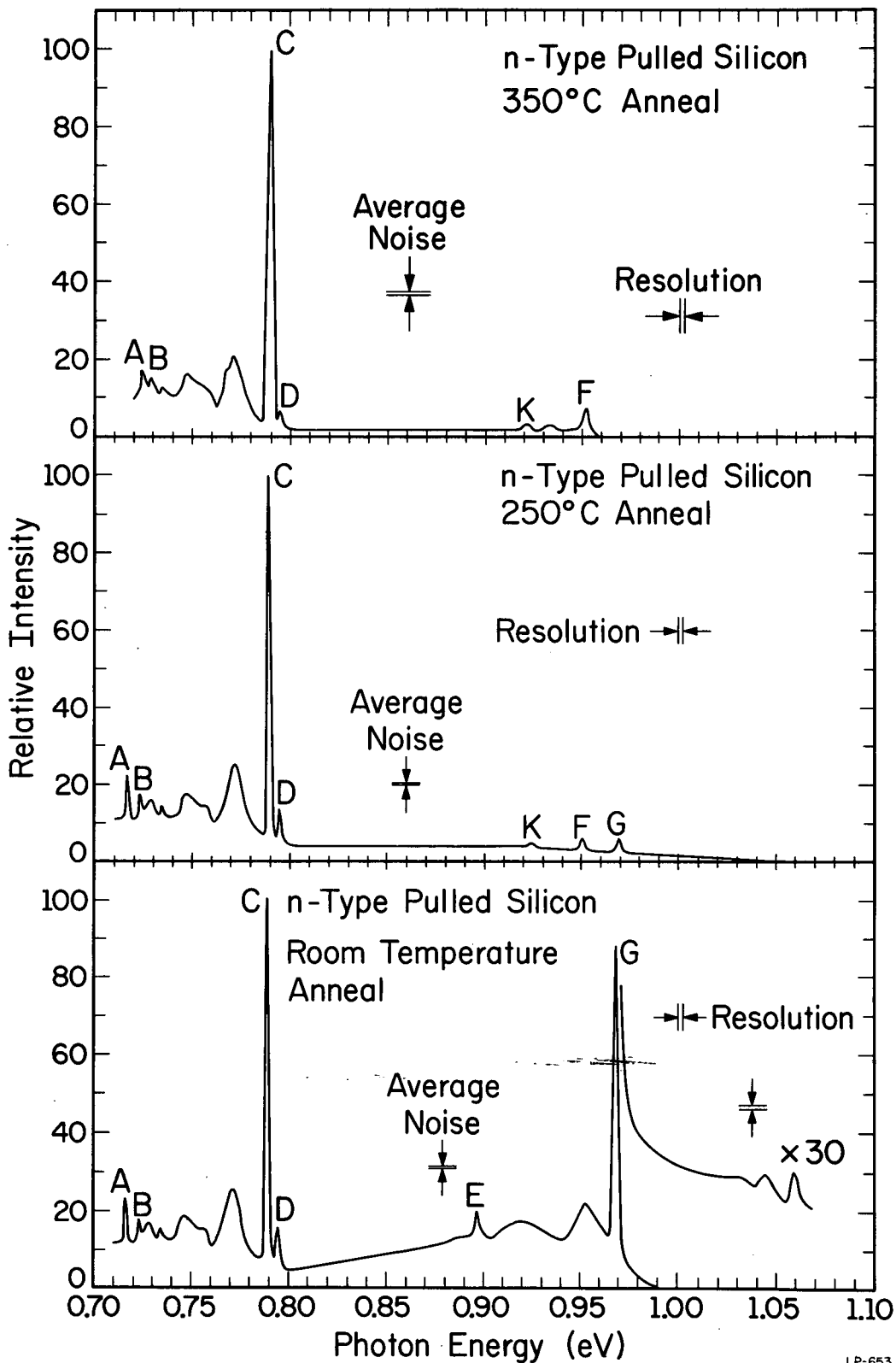
Figure 14. Luminescence spectra from n-type pulled silicon irradiated to a fluence of 10^{17} e/cm². The full spectra shown were observed after twenty-minute room temperature (23°C), 250, and 350°C anneals. A partial spectrum shows the structure at high energy under high gain. The partial spectrum has been translated vertically. The spectra were observed near liquid helium temperature.
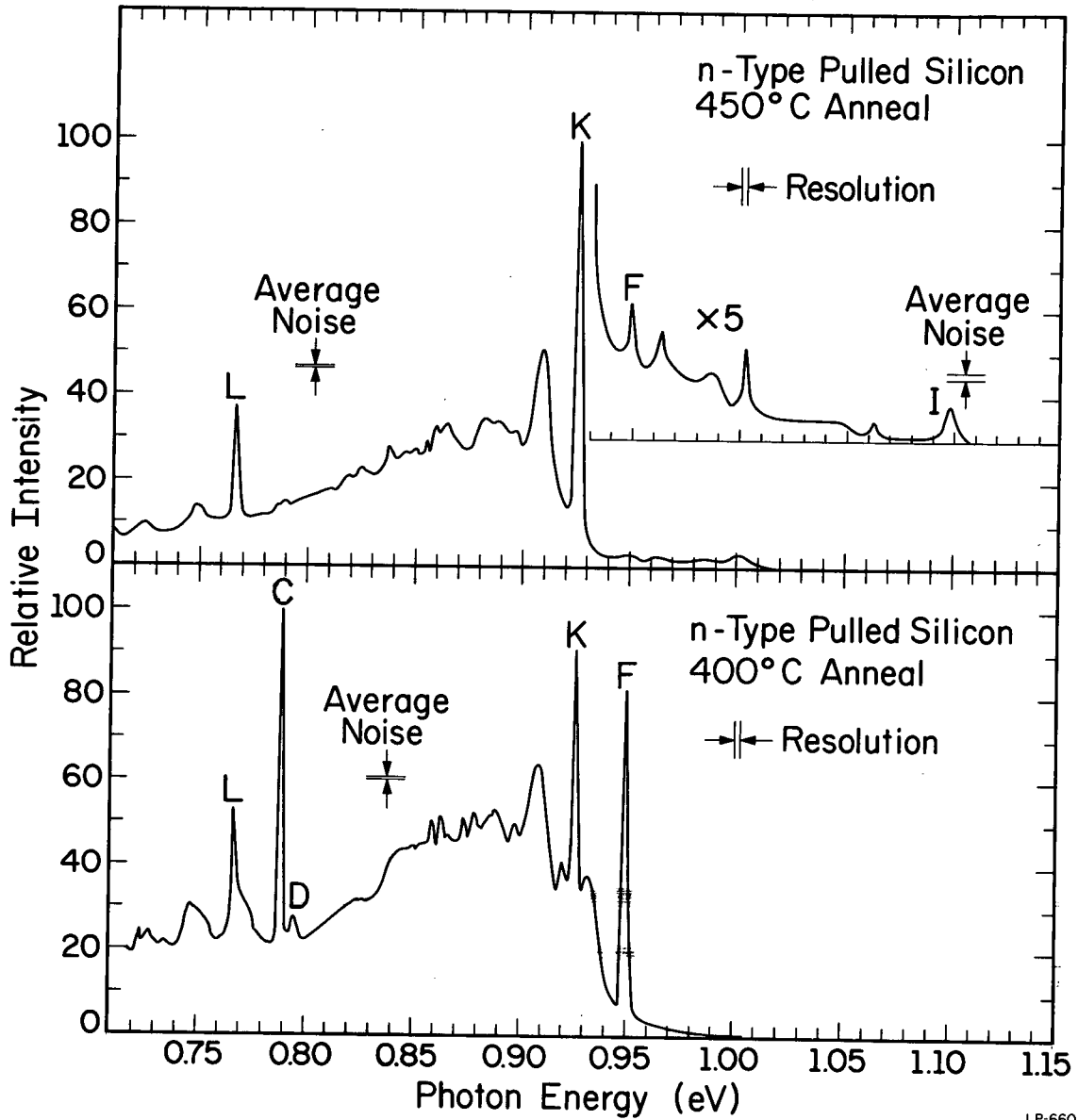
Figure 15. Luminescence spectra from n-type pulled silicon irradiated to a fluence of 10^{17} e/cm^2. The sample was previously annealed in the temperature range 23 to 350°C. (See Fig. 14) The full spectra shown here were obtained after additional twenty-minute anneals at 400°C and 450°C. A partial spectrum of weak luminescence at high energy observed following 450°C anneal is shown in the upper figure. The spectra were observed near liquid helium temperature.

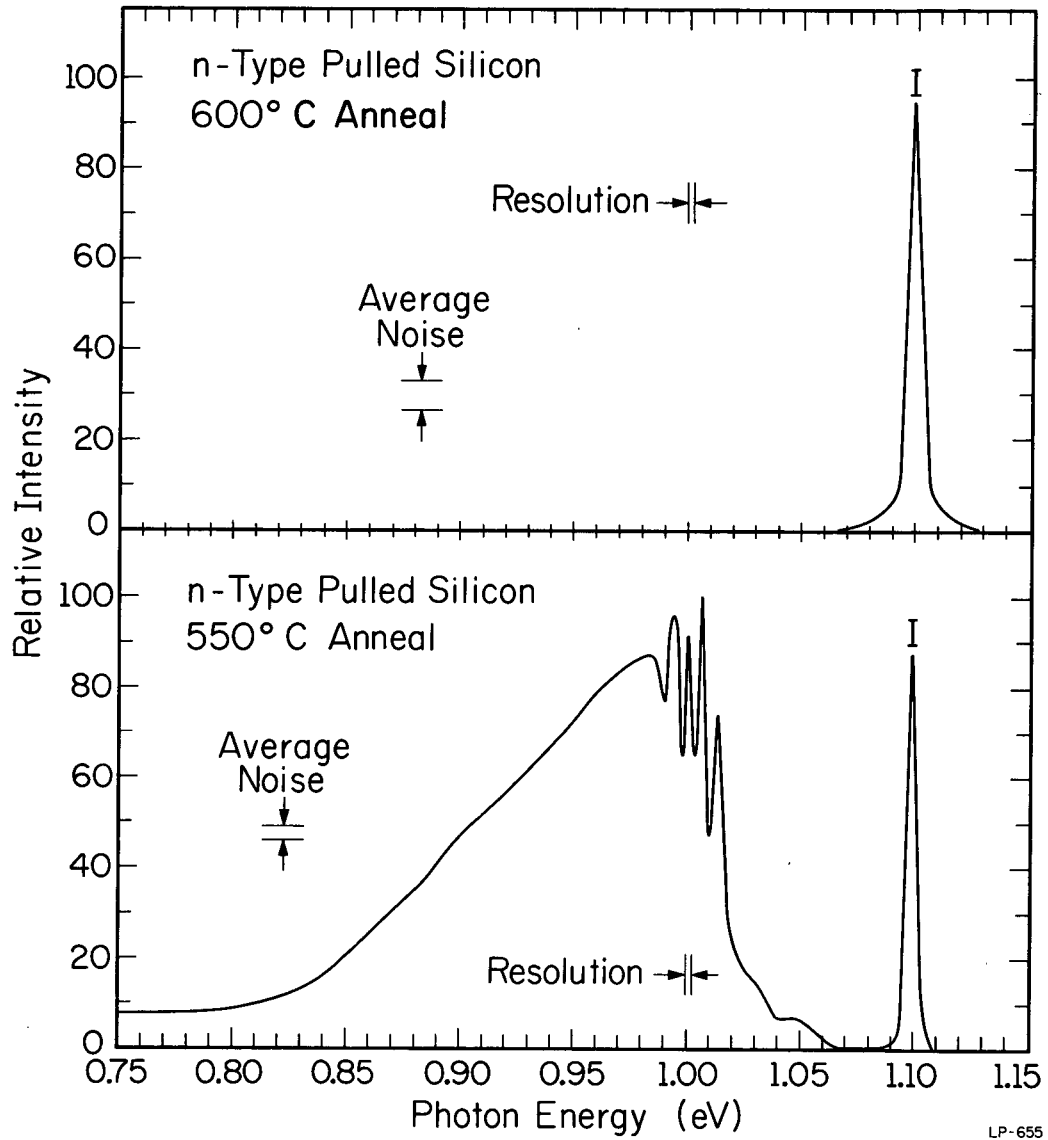Figure 16. Luminescence spectra from n-type pulled silicon irradiated to a fluence of 10^{17} e/cm^2. The sample was previously annealed in the temperature range 23 to 450°C (See Figs. 14 and 15). The spectra shown here were obtained after additional twenty-minute anneals at 550°C and 600°C. The spectra were observed near liquid helium temperature.

$500^{o}C$ anneal. The bottom of Fig. 16 shows a spectrum of unusual structure accompanying the intrinsic luminescence following $550^{o}C$ anneal. Only weak intrinsic luminescence was seen following $600^{o}C$ anneal. The intensity of the intrinsic luminescence remained at 3% of the preirradiation value through anneal to $700^{o}C$.

The isochronal annealing of the prominent zero-phonon peaks observed in n-type pulled silicon is shown in Fig. 17. Annealing curves are shown for peaks C (0.79 eV), G (0.97 eV), F (0.950 eV), K (0.925 eV), and L (0.767 eV). The observed intensities were normalized to the maximum intensity of peak C.

Isothermal annealing data for peak G (0.97 eV) is shown in Fig. 18. The annealing follows first-order kinetics. The calculated activation energy for this annealing is approximately 1.3 eV.

3.2.4. p-Type Pulled Silicon

Spectra from p-type pulled silicon annealed in the temperature range 23 to $600^{o}C$ are shown in Figs. 19, 20, and 21. The spectra were very similar to those seen in n-type pulled silicon, with the following exceptions: The intensity of peak C (0.79 eV) was reduced relative to peak G (0.97 eV) following anneal at room temperature (bottom Fig. 19); on no occasion was structure observed in the room temperature pretail; the intensity of zero-phonon peaks F, K, and L was reduced; a new zero-phonon peak, M, at 0.760 eV, was observed in the $350^{o}C$ anneal spectrum (bottom Fig. 20); the weak spectra observed after $500^{o}C$ and $550^{o}C$ anneal are unique to p-type pulled silicon (bottom Fig. 21); and, the intrinsic luminescence intensity returned to a value approximately equal to the

n-Type Pulled Silicon
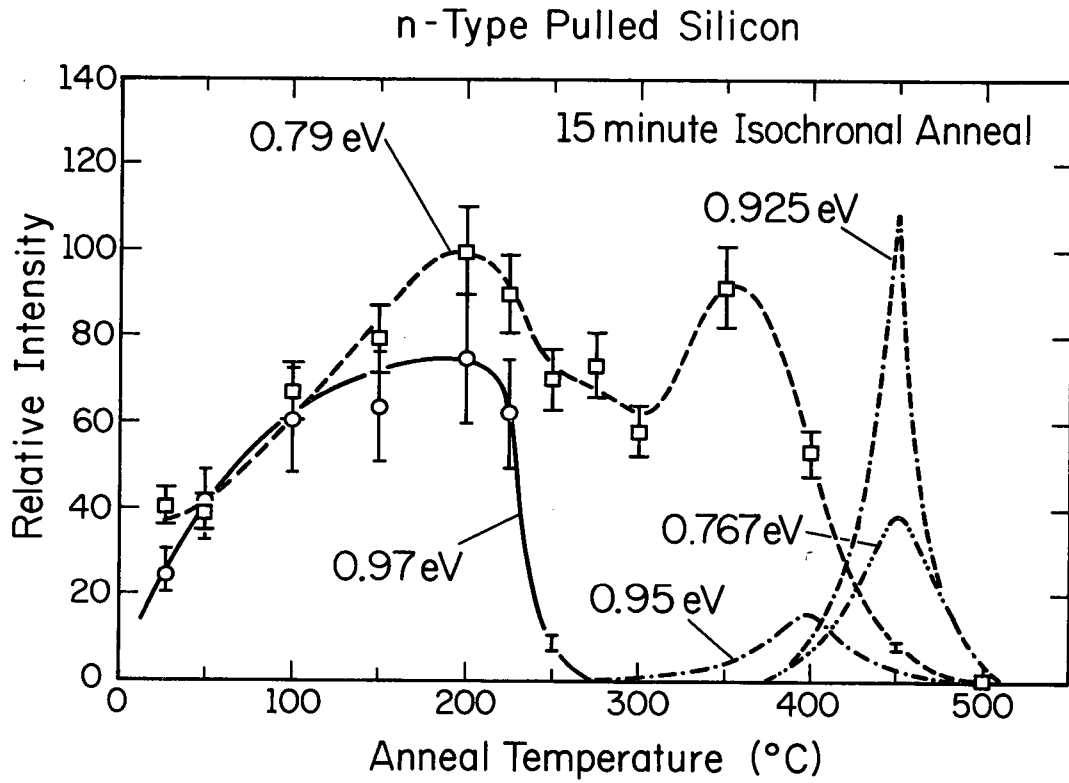
LS-666

Figure 17. The isochronal annealing of zero-phonon peaks C (0.79 eV), G (0.97 eV), F (0.950 eV), K (0.925 eV), and L (0.767 eV), in n-type pulled silicon.
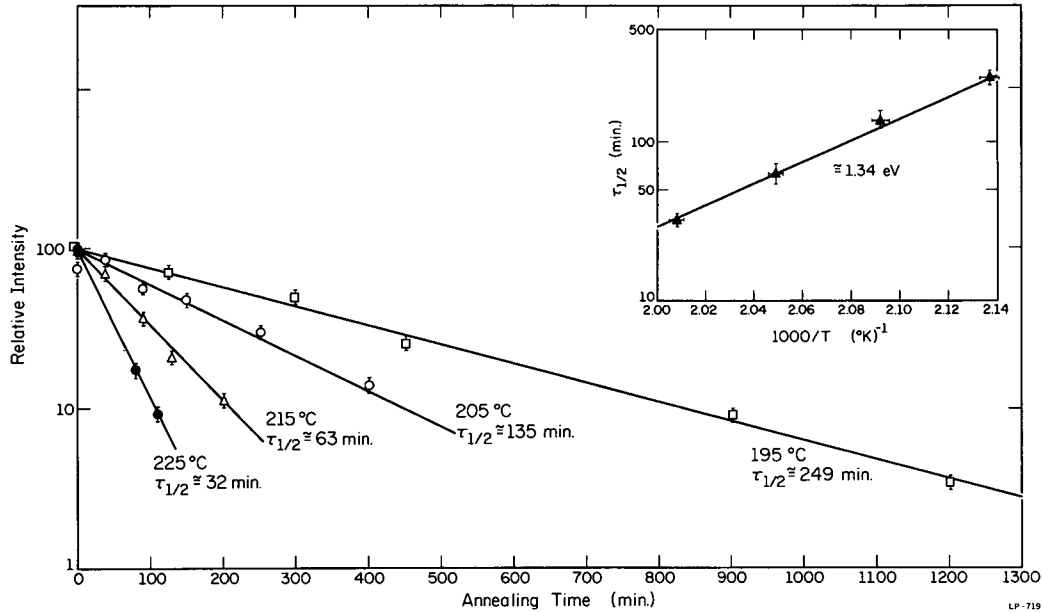
Figure 18. Isothermal annealing of the 0.97 eV zero-phonon line in n-type pulled Si after irradiation with 3 MeV electrons to a fluence of 10^{18} electrons/cm^2. The inset shows the temperature dependence of the time to half recovery ($\tau_{1/2}$) for calculation of the activation energy.

Figure 19. Luminescence spectra from p-type pulled silicon irradiated to a fluence of 10^{17} e/cm^2. The full spectra shown were observed after twenty-minute room temperature (23°C) and 250°C anneals. Partial spectra at high gain of the luminescence at high energy are shown in the bottom of the figure. The spectra were observed near liquid helium temperature.

Figure 20. Luminescence spectra from p-type pulled silicon irradiated to a fluence of 10^{17} e/cm^2. The sample was previously annealed in the temperature range 23 to 250°C (See Fig. 19). The spectra shown here were obtained after additional twenty-minute anneals at 350, 450, and 500°C. The spectra were observed near liquid helium temperature.

Figure 21. Luminescence spectra from p-type pulled silicon irradiated to a fluence of 10^{17} e/cm^2. The sample was previously annealed in the temperature range 23 to 500°C (See Fig. 20 and 21). The spectra shown here were obtained after additional twenty-minute anneals at 550°C and 600°C. The spectra were observed near liquid helium temperature.

preirradiation value following anneal at 700°K.

The isochronal annealing curves of prominent zero-phonon peaks observed in p-type pulled silicon are shown in Fig. 22. The peaks shown are C (0.79 eV), G (0.97 eV), F (0.950 eV), K (0.925 eV), L (0.767 eV), and M (0.760 eV). The observed intensities were normalized to the maximum intensity of peak G.

One must consider the possibility that the luminescence observed following high-temperature annealing arose not from defects induced by irradiation but from thermally introduced defects; this possibility led to an examination of the spectra of unirradiated annealed silicon. The following unirradiated samples were examined after annealing and routine quenching from the indicated temperatures: n-type float zone - 400°C; p-type float zone - 450, 500, and 600°C; and, n-type pulled - 500°C. In each case, only intrinsic luminescence was observed.

3.2.5. Summary

The threshold fluence for most materials was between 10^{16} e/cm^2 and 10^{17} e/cm^2. Only in the case of n-type pulled silicon was it appreciably lower (10^{14} e/cm^2).

The intensity of peak G (0.97 eV) following room temperature anneal was lower by a factor of 5 to 15 in float zone silicon than it was in pulled silicon. The maximum intensities of peak G obtained during the annealing sequences were similar for float zone and pulled silicon.

Luminescence of energy greater than 0.97 eV found following room temperature anneal was more prominent in float zone silicon than in pulled silicon; it was more prominent in p-type than in n-type
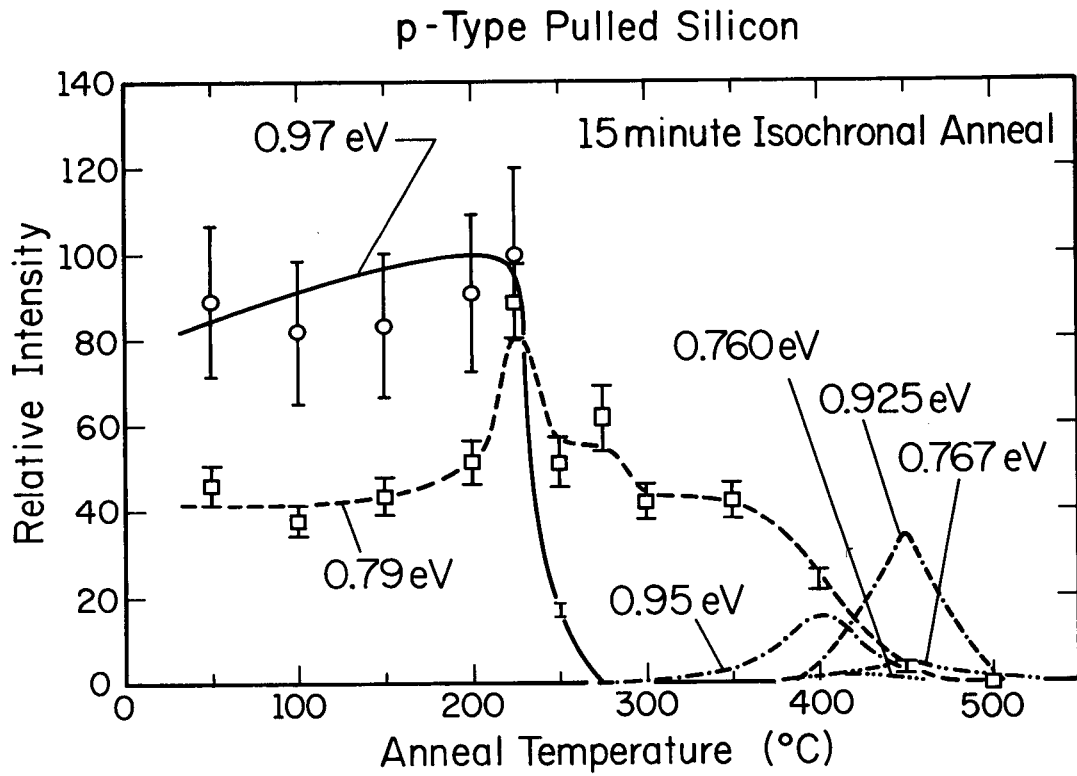
Figure 22. The isochronal annealing of zero-phonon peaks C (0.79 eV),
G (0.97 eV), F (0.950 eV), K (0.925 eV), L (0.767 eV), and
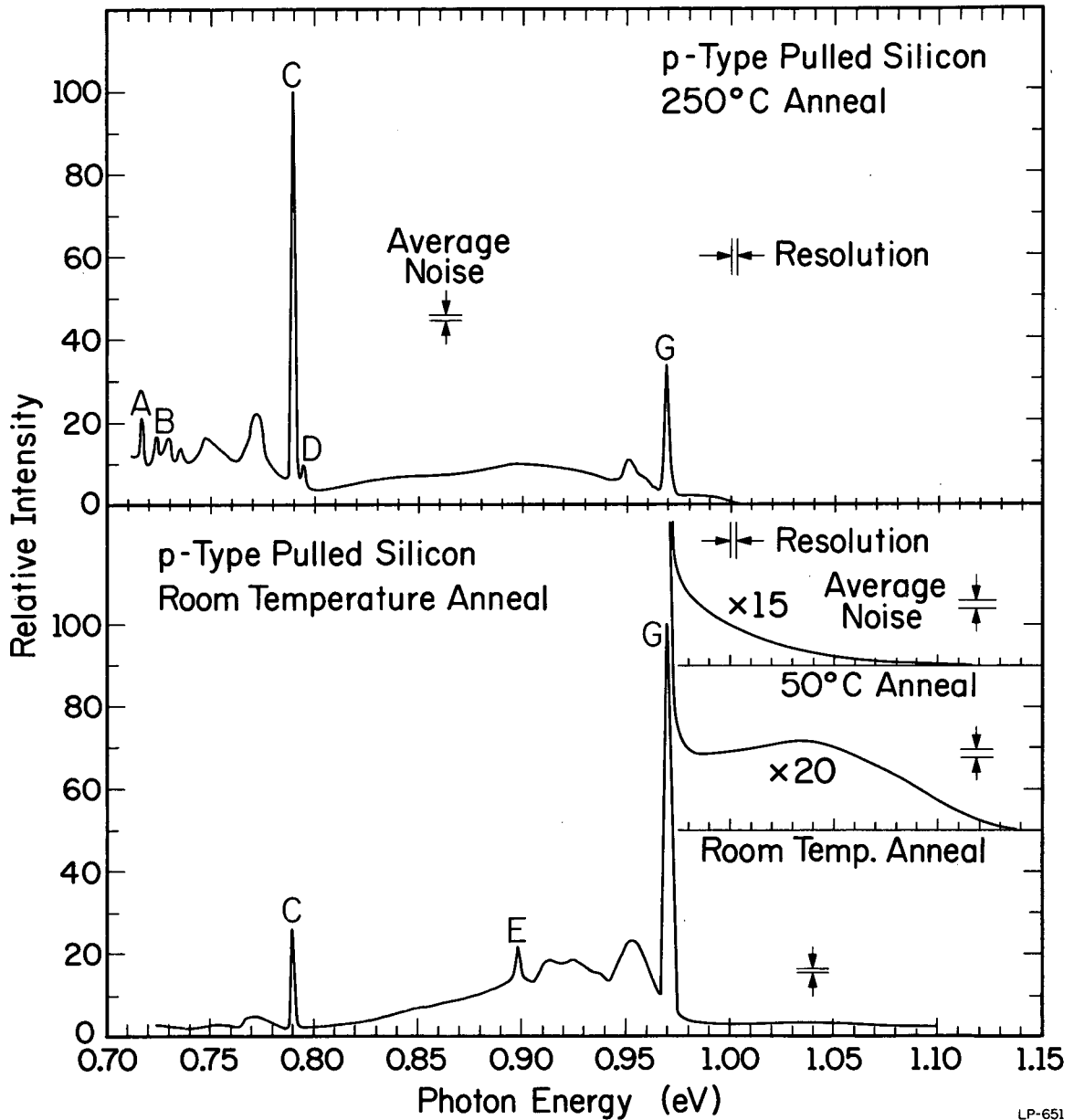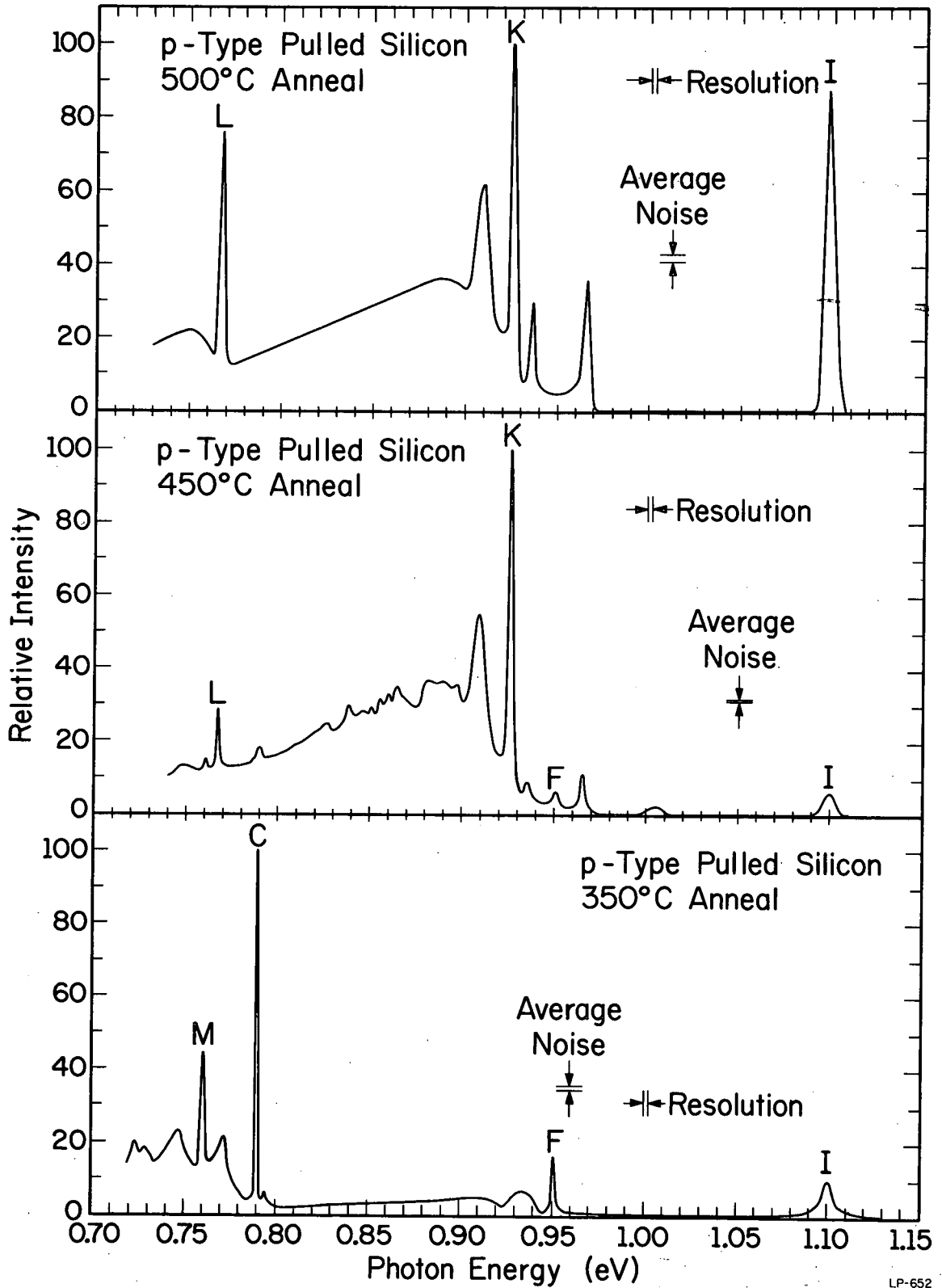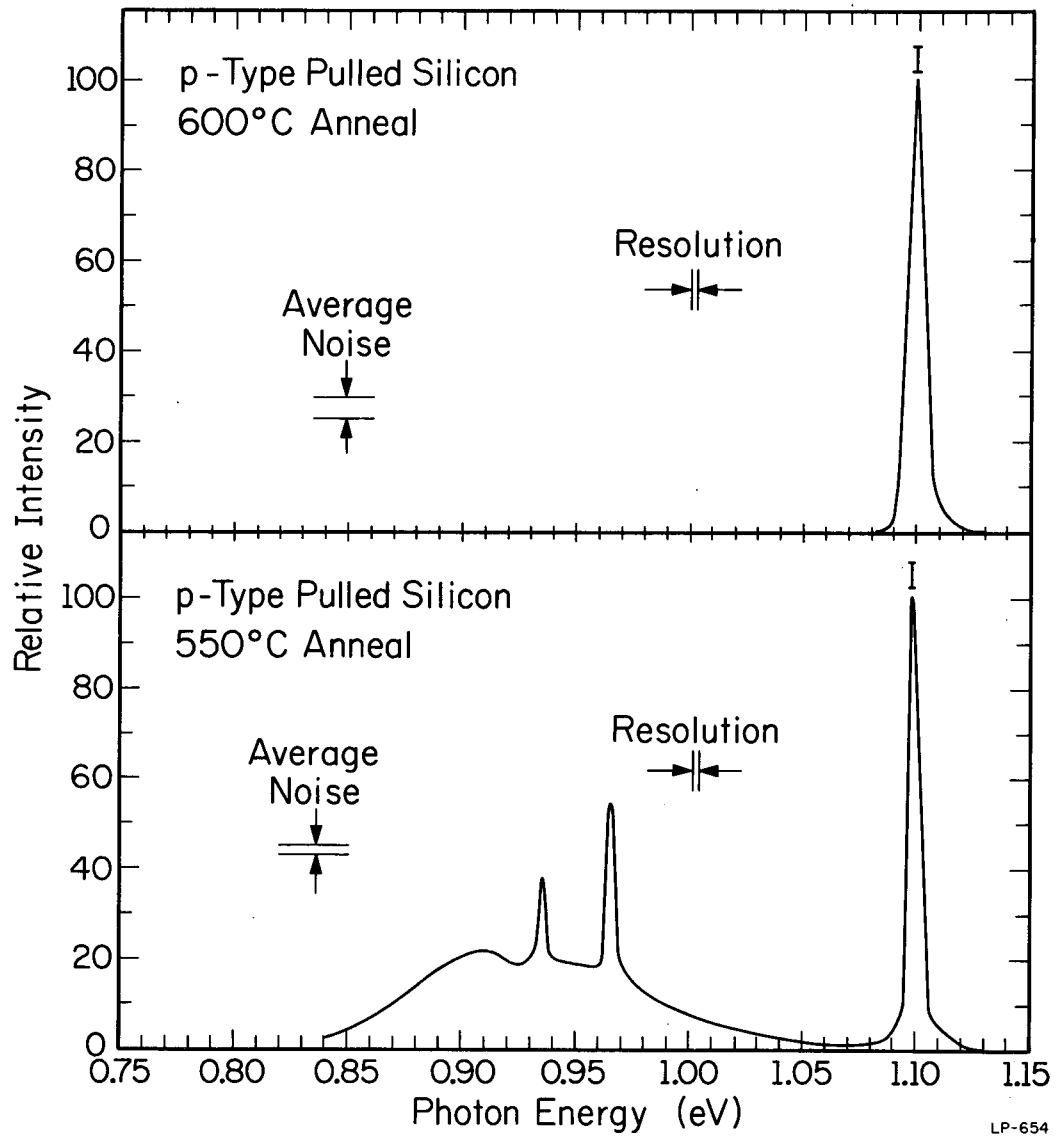M (0.760 eV), in p-type pulled silicon.

silicon.

Peak G (0.97 eV) annealed out between 300°C and 325°C in float zone silicon, and vanished at 275°C in pulled silicon.

Peak C (0.79 eV) had a broad annealing stage that began between 250° and 350°C and was not completed until about 500°C.

Peak J was the only prominent zero-phonon peak found in p-type float zone silicon during high temperature anneal (to 500°C).

Peaks F, K, L, and M were observed during high temperature anneal of pulled silicon (to 500°C).

In general, irradiation-induced luminescence was quenched or very weak following anneal at temperatures between 500°C and 600°C.

Annealing above 600°C produced complex spectra in float zone silicon; only intrinsic luminescence was observed from pulled silicon annealed at this temperature.

3.3. Lithium-Diffused Silicon

The lithium-diffused silicon used in this investigation was always n-type after diffusion due to the large concentration of lithium donors. When reference is made to p- or n-type lithium-diffused silicon in the following sections one means the conductivity type prior to lithium diffusion.

Intrinsic luminescence associated with free exciton recombination was observed at low intensity in unirradiated lithium-diffused silicon. This result was somewhat unexpected because most of the lithium samples examined had electrically-active lithium concentrations on the order of the impurity concentration for which Haynes reported bound exciton

spectra. Furthermore, it appeared that the position of the strong TO

line shifted to higher wavelength with increasing lithium concentration.

The maximum shift observed was 200 $\overset{\circ}{A}$ for a lithium concentration of 10^{18}

atoms/cm^3. No shift was observed for a lithium concentration of $3 \cdot 10^{16}$

atoms/cm^3.

3.3.1. Lithium-Diffused Float Zone Silicon

It is difficult to use the concept of threshold fluence, as

previously defined, in the case of lithium-diffused silicon for two

reasons. First, the intrinsic luminescence was observed to vanish without

the appearance of strong defect luminescence, and second, there was some

evidence that the fluence at which the intrinsic luminescence vanished

depends on the lithium concentration. In spite of these drawbacks, some

general comments concerning fluence can be made. Intrinsic·luminescence

vanished after a fluence of about 10^{16} e/cm^2. Weak luminescence attributed

to irradiation-induced defects was seen following irradiation to a fluence

of 10^{17} e/cm^2; strong defect luminescence was consistently produced by an

irradiation fluence of 10^{18} e/cm^2.

The luminescence spectrum from irradiated lithium-diffused float

zone silicon after room temperature annealing is shown in Fig. 23. This

spectrum is dominated by zero-phonon peak Q at 1.045 eV and shows no resem-

blance to the spectra observed in non-lithium-doped float zone silicon.

However, peak G (0.97 eV) was occasionally observed as a small peak super-

imposed on the spectrum of Fig. 23. Peak G was most commonly observed in

lithium-doped samples with low lithium concentrations ($\sim 10^{16}$ atoms/cm^3),

but no single parameter affecting its appearance could be determined.
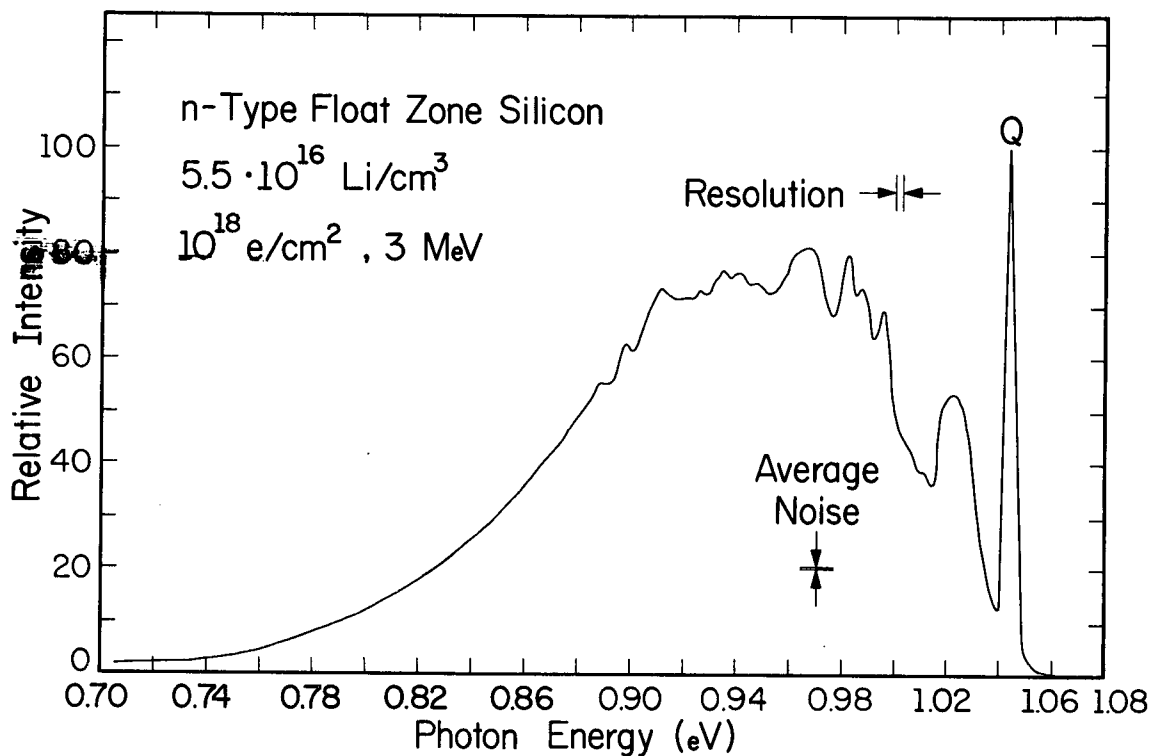
Figure 23. Luminescence spectrum typical of lithium-diffused n- or
p-type float zone silicon irradiated to a fluence of 10^{18}
e/cm^2. The sample used to obtain this spectrum had a
lithium concentration of $5.5 \cdot 10^{16}$ atoms/cm^3. This spectrum
is associated with the recombination center responsible
for zero-phonon peak Q at 1.045 eV. The spectrum was
observed at 12.8°K.

Figure 24 shows a portion of the spectrum shown in Fig. 23 taken with higher resolution. This higher-resolution spectrum reveals a number of weak peaks which seemed to be as sharp as Q and do not appear to involve phonon cooperation. These peaks are designated N (0.990 eV), O(0.997 eV), P (1.013 eV) and R (1.045 eV) in Fig. 24. An additional zero-phonon peak appears to exist at 0.9825 eV. Further investigations cast doubt on this assignment and the correct assignment remains an open question.

Consistent isochronal annealing of peak Q was not possible. The intensity of this peak was found to increase as a function of anneal temperature in some samples and to decrease over the same temperature range in others. Undoubtedly, lithium concentration is of tremendous importance. The temperature at which a defect vanishes should be a property of the defect, whereas intensity variations at lower annealing temperatures will depend on competitive processes. Therefore, the determination of an annealing temperature is reasonably significant. The defect associated with peak Q (1.045 eV) was found to anneal out between $400^{\circ}C$ and $450^{\circ}C$ in n-type float zone silicon. Peaks N, O, P, and R maintained a constant ratio with peak Q and annealed out in the same temperature range. Therefore, the entire spectrum shown in Fig. 24 can be assumed to be due to a single defect.

Figure 25 is a composite of the spectra observed from annealed lithium-diffused n-type float zone silicon. The room temperature spectrum (bottom Fig. 25) and its annealing have already been discussed. New zero-phonon peaks S (0.947 eV), T (0.970 eV), and U (1.025 eV) appeared
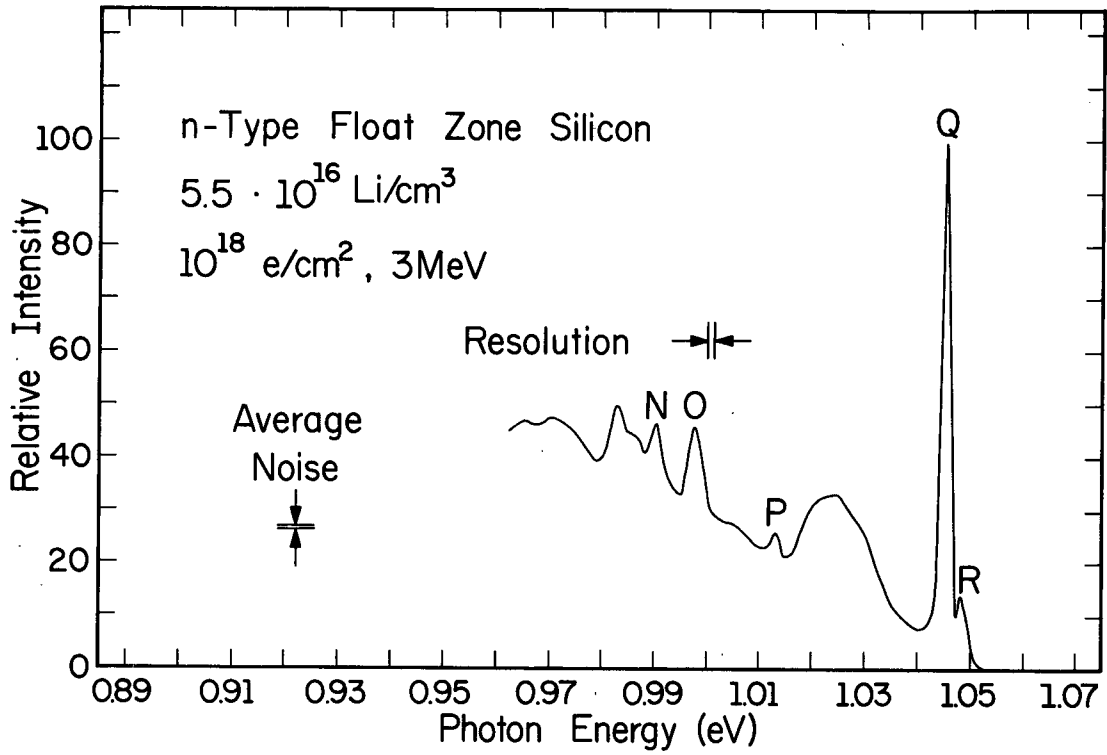
Figure 24. Luminescence spectrum from lithium-diffused n-type float
zone silicon irradiated to a fluence of 10^{18} e/cm^2. The
monochromator resolution is 16 Å. Weak zero-phonon peaks
N (0.990 eV), O (0.977 eV), P (1.013 eV), and R (1.048 eV)
are shown. The spectrum was observed at 14.2°K.
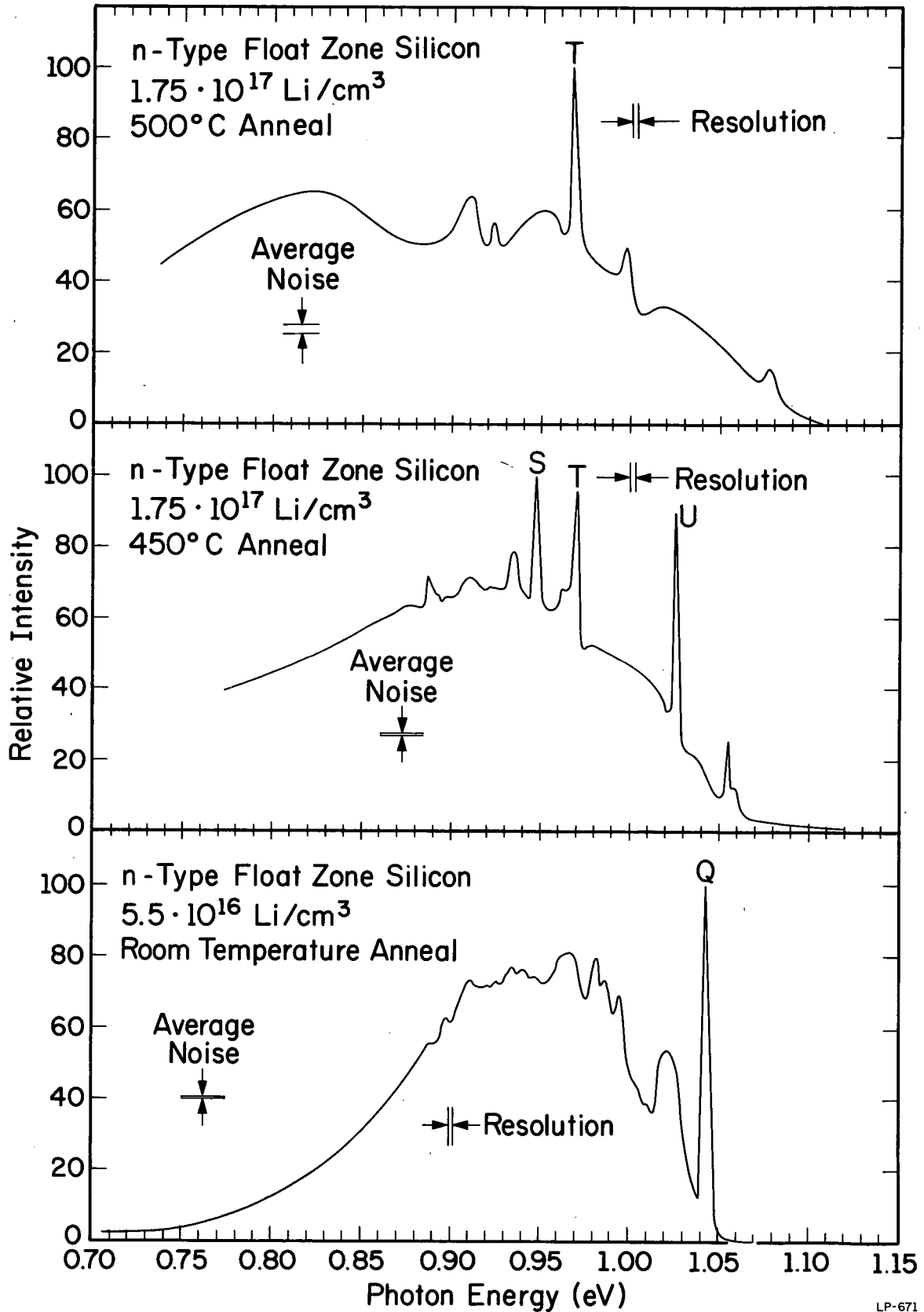
Figure 25. Luminescence spectra from lithium-diffused n-type float zone silicon irradiated to a fluence of 10^{18} e/cm^2. Spectra observed after twenty-minute room temperature (23°C), 450, and 500°C anneals are shown. The spectra were observed near liquid helium temperature.

following 450°C anneal. Peaks S and U vanished following 500°C anneal

and only the weak peak T remained. The annealing of p-type float zone

silicon was taken to 200°C and no changes in the spectrum shown in Fig. 23

were observed.

3.3.2. Lithium-Diffused Pulled Silicon

Figure 26 shows the spectrum of irradiated lithium-diffused n-type

pulled silicon following room temperature anneal. The dominant luminescence

observed was characteristic of the 0.97 eV defect; traces of peaks C and Q

were also observed in addition to a broad peak at low energy. Additional

structure, not seen in lithium-free n-type pulled silicon, was observed

between peaks C and E.

Luminescence spectra from irradiated lithium-diffused p-type

pulled silicon annealed in the temperature range 23 to 600°C are shown

in Fig. 27, 28 and 29. Only luminescence associated with zero-phonon peaks

C and G was observed following room temperature anneal (bottom Fig. 27).

New zero-phonon lines V (0.785 eV) and W (0.878 eV) grew in slowly during

successive anneals at 100°C (top Fig. 27), 200°C (bottom Fig. 28), and

300°C (middle Fig. 28). Peak Q was observed following 200°C anneal and

vanished following 350°C anneal. Further annealing at 400°C (top Fig. 28)

and 500°C (bottom Fig. 29) produced peak X (1.001 eV). Weak luminescence

with little structure was observed following 600°C anneal.

The annealing of zero-phonon peaks G and C is of interest in

lithium-diffused silicon. Peak G annealed out near 300°C, a result

consistent with results for lithium-free silicon. Peak C, however,

annealed out near 400°C, which is roughly 100°C lower than its annealing

Figure 26. Luminescence spectrum from lithium-diffused n-type pulled silicon irradiated to a fluence of 10^{18} e/cm^2 and annealed for twenty-minutes at room temperature (23°C). Zero-phonon peaks which may be recognized are C, E, G, and Q. The spectrum was observed at 16.4°K.
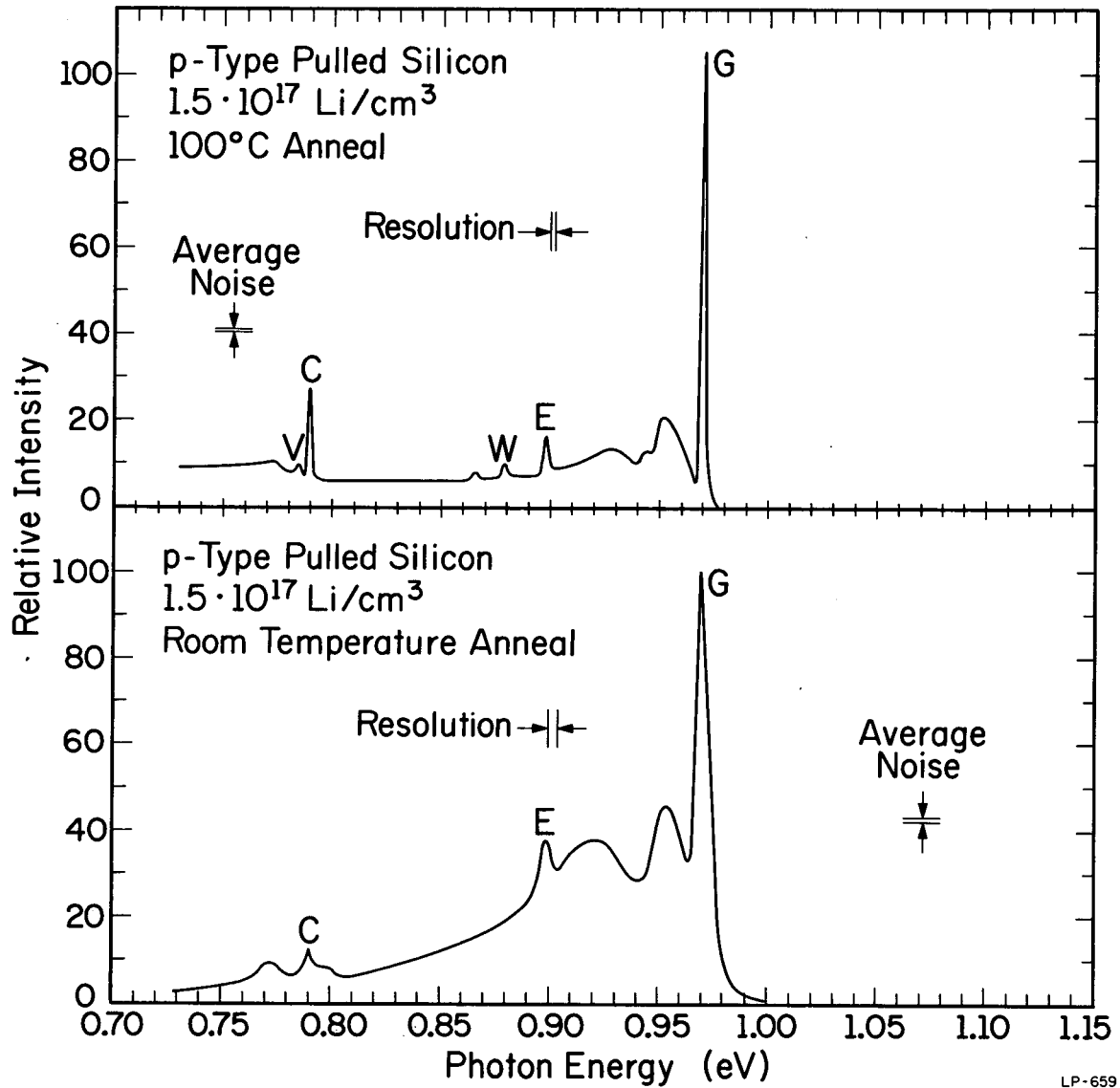
Figure 27. Luminescence spectra from lithium-diffused p-type pulled silicon irradiated to a fluence of 10^{18} e/cm^2. Spectra observed after twenty-minute room temperature (23°), and 100°C anneals are shown. The spectra were observed near liquid helium temperature.

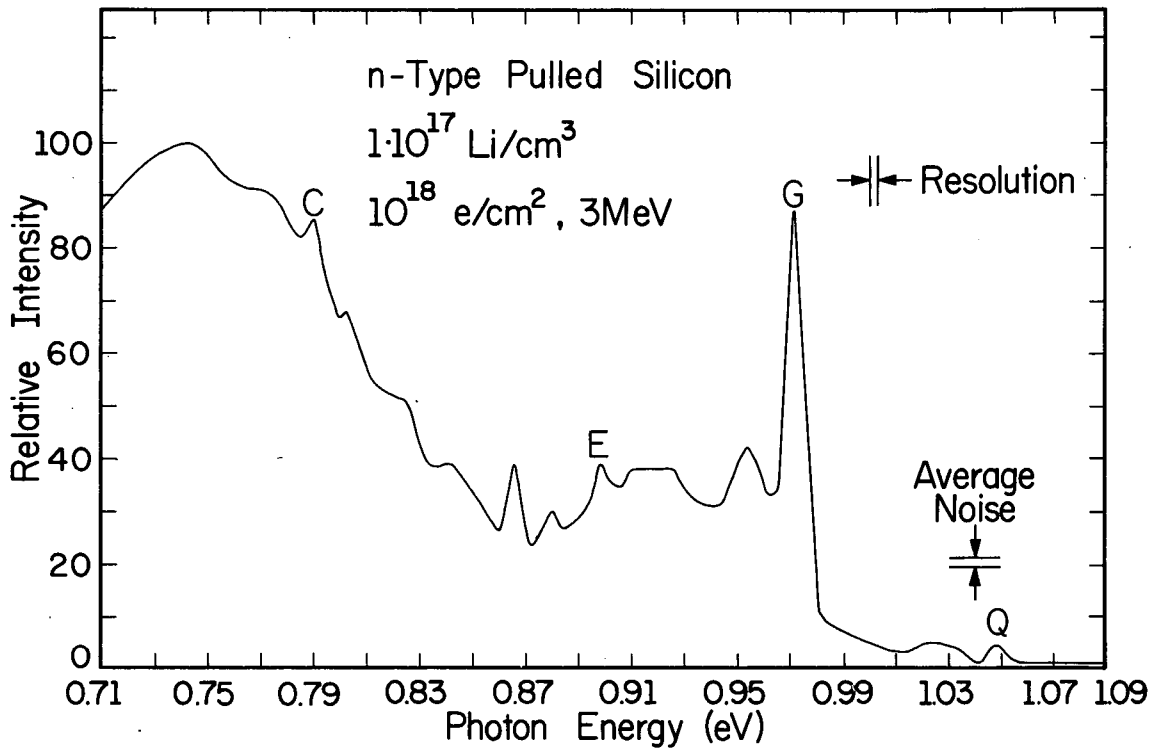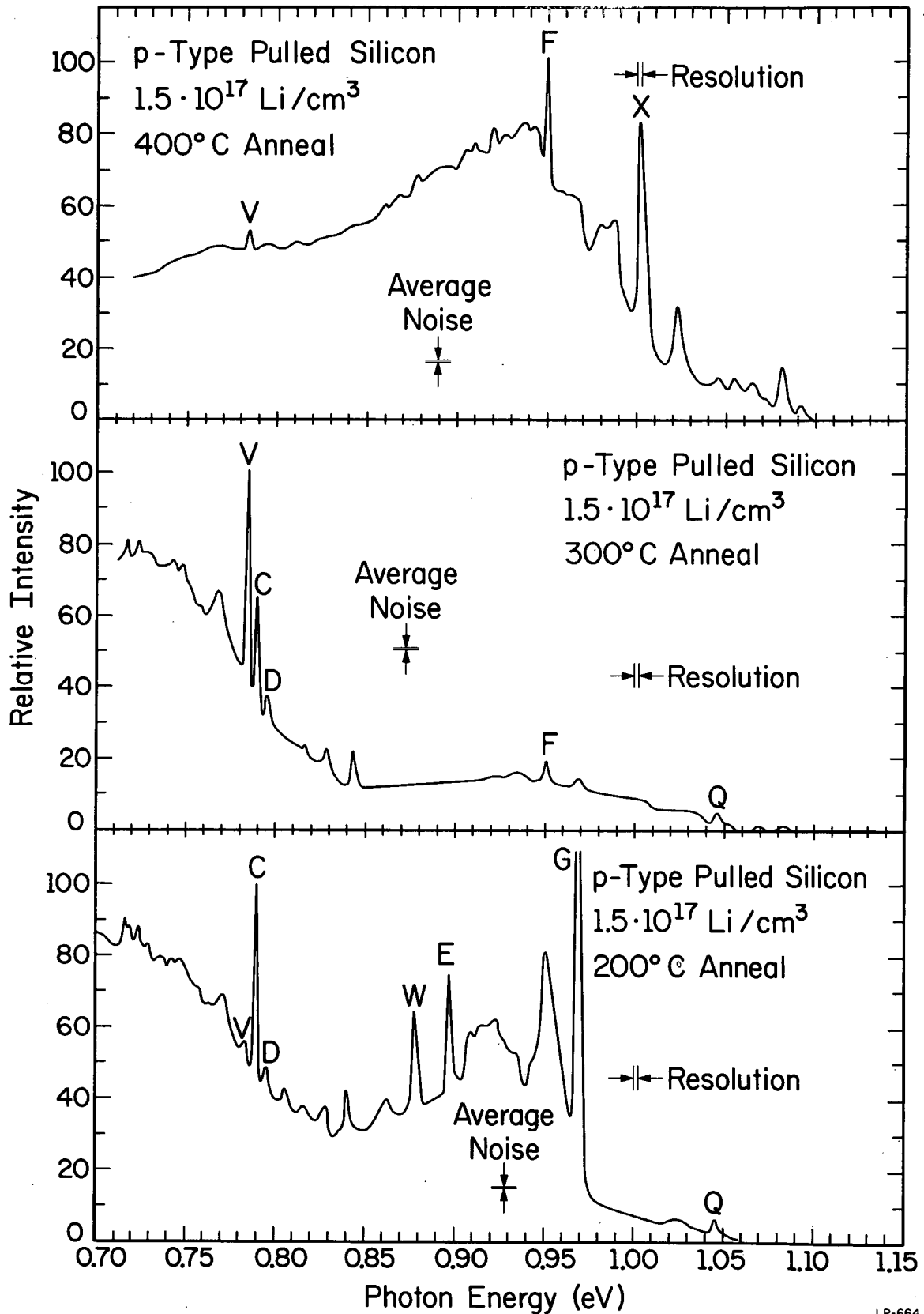Figure 28. Luminescence spectra from lithium-diffused p-type pulled silicon irradiated to a fluence of 10^{18} e/cm^2. The sample was previously annealed in the temperature range 23 to 100°C (See Fig. 27). Spectra shown here were observed following successive 200, 300, and 400°C anneals. The spectra were observed near liquid helium temperature.
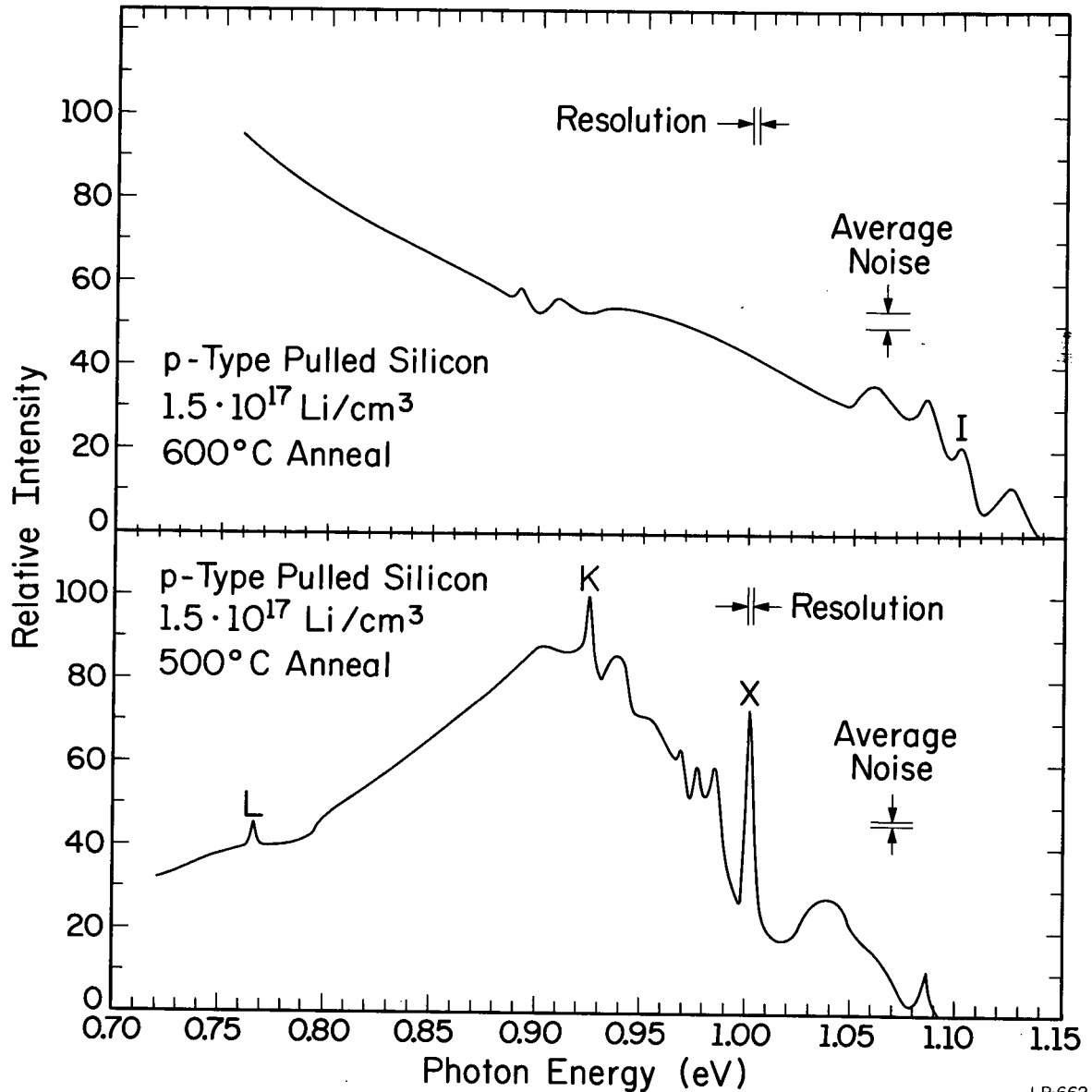
Figure 29. Luminescence spectra from lithium-diffused p-type pulled silicon irradiated to a fluence of 10^{18} e/cm^2. The sample was previously annealed in the temperature range 23 to 400°C (See Figs. 27 and 28). Spectra shown here were observed following successive 500°C and 600°C anneals. The spectra were observed near liquid helium temperature.

temperature in lithium-free pulled silicon. In addition, peaks F, K, and L, appeared in lithium-diffused pulled silicon at approximately the same temperature as they did in lithium-free silicon.

The annealing characteristics of lithium-diffused n- and p-type pulled silicon were similar up to 350°C. The major difference was that the weak lithium-dependent peaks seen in p-type silicon following anneal at 200°C appeared in n-type silicon after room temperature anneal. The intensity of the peaks in n-type material was different from peaks observed in p-type silicon, however. Nevertheless, the energy agreement of the peaks suggested this is a population effect and not a result of different defects.

3.3.3. Summary of Lithium-Diffused Silicon Spectra

Intrinsic luminescence was generally quenched after irradiation to a fluence of 10^{16} e/cm^2; strong defect-luminescence spectra were observed after irradiation to a fluence of 10^{18} e/cm^2.

Luminescence involving a center which is dependent on lithium for its formation was observed in irradiated lithium-diffused float zone silicon annealed at room temperature. Peak Q (1.045 eV) was the dominant zero-phonon peak in this spectrum, but weak zero-phonon peaks N, O, P, and R were also associated with this center. The center annealed out near 400°C.

Zero-phonon peaks S, T, and U were observed in lithium-diffused n-type float zone silicon at anneal temperatures between 450°C and 500°C.

Luminescence spectra from irradiated lithium-diffused pulled silicon presented a mixture of lithium-dependent centers and centers seen in lithium-free silicon. Centers associated with lithium-free silicon, such as G and C, were more prominent in p-type than in n-type lithium-

diffused silicon for annealing temperatures less than 200°C. Zero-phonon peaks Q, V, W, and X were dependent upon lithium for their formation. The intensity of zero-phonon peak Q, the dominant luminescent peak in irradiated lithium-diffused float zone silicon, was always relatively weak in pulled silicon.

3.3.4. The Nature of the Dominant Lithium-Dependent Center

The spectrum shown in Fig. 23 was always observed as a unit; it was also observed to anneal out as a unit. This spectrum was therefore attributed to recombination at a single center. Data on the properties of the prominent zero-phonon peak at 1.045 eV, which provide detailed information of the microscopic properties of this center, are discussed here.

Most of the data on the temperature-dependent properties of peak Q were taken using a sample of lithium-diffused p-type float zone silicon (lithium concentration $7 \cdot 10^{16}$ atoms/cm^3) which had been irradiated to a fluence of 10^{18} e/cm^2. Maximum intensity was observed at 14°K, with an approximately exponential decrease at higher temperature.

Measurements of the half-widths as a function of temperature for zero-phonon peaks Q and R exhibit sublinear temperature dependencies as was the case for peaks C and G (see for example, Fig. 6). The broadening for peak Q varies approximately as $T^{2.1}$. A log-log plot of the broadening for peak R as a function of temperature does not give a straight line. A log-log plot of the shift in the position of peak Q as a function of temperature gives a straight line with a slope of 2.78 ± 0.5. Therefore, the shift varies approximately as $T^{2.8}$.

The separation between zero-phonon peaks Q and R increased linearly with temperature. The closest separation, extrapolated to T = 0°K, was 33.6 Å. This separation corresponds to an energy of 2.96 meV; at 70°K the separation was 3.18 meV.

3.4. Stressed Samples

Samples with and without lithium doping were stressed along crystallographic directions and the effects of this stress on the luminescence spectra were measured. The narrow half-widths of the zero-phonon lines made it possible to measure shifts and splitting produced by stress. The most extensive stress measurements were made on the strong C line at 0.79 eV, the G line at 0.97 eV, and the Q line at 1.045 eV (in lithium-doped material).

As an example of these results, Fig. 30 shows the stress dependence of the 0.79 eV peak for various stress directions. Both shifting and splitting of the peak is evident in this figure. Summaries of the stress data for peaks Q, C, and G are represented schematically in Figs. 31 to 33. Included in these figures are the effects of polarization.

C.2

No Stress

[100] Stress
T = 20° K

Res.
Noise

[011] Stress
[01Ī] View
T = 32° K

Res.
Noise

[111] Stress

Relative Intensity

0.790   0.795   0.800

Photon Energy (eV)

LR-550
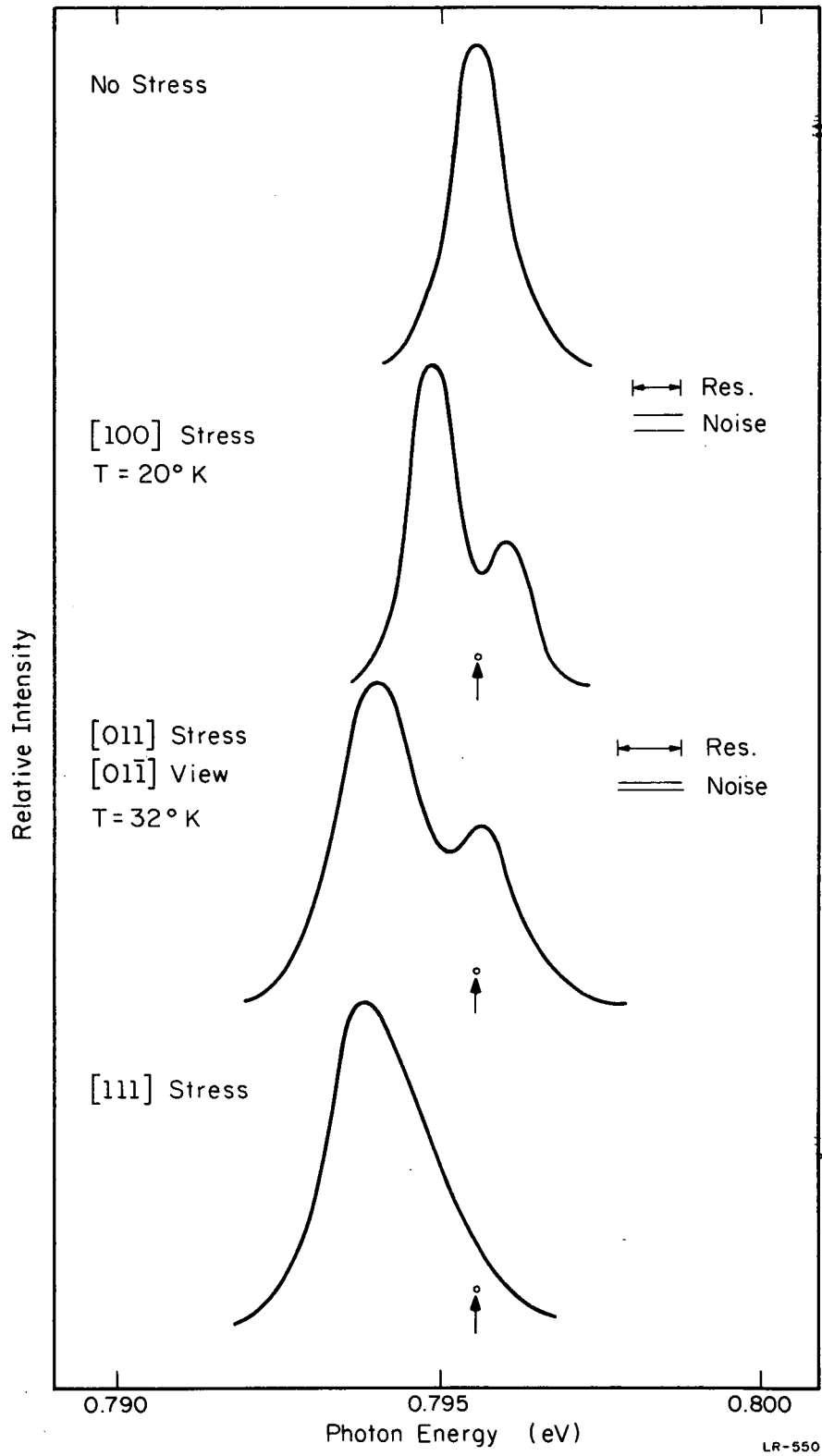
Figure 30.   Stress dependence of peak C at 0.796 eV.   The arrow marks
the zero stress position.

Peak Q at 1.045 eV
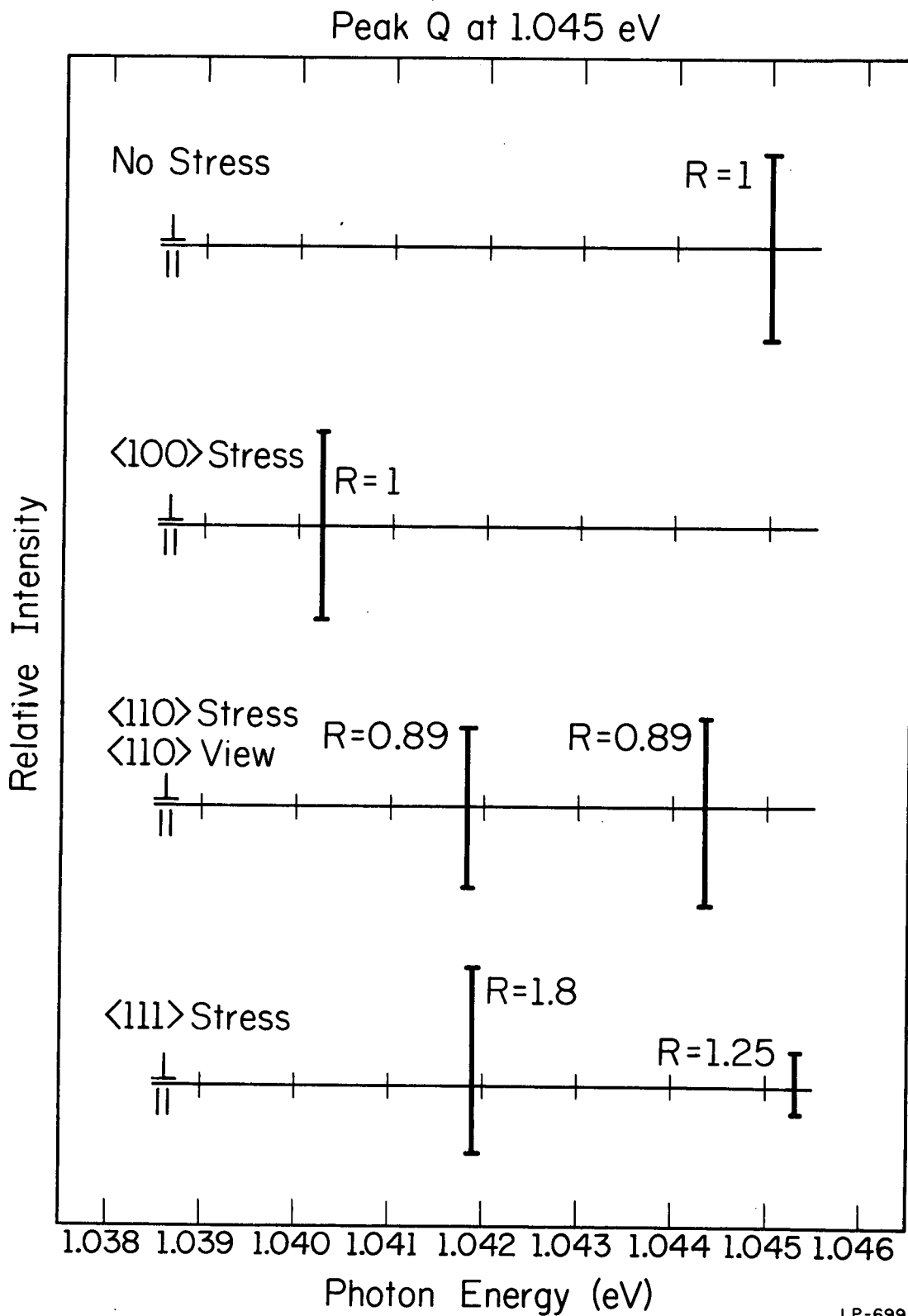
Figure 31. Representation of the stress splittings and polarization of zero-phonon peak Q (1.045 eV). The quantity $R = I_\perp/I_{\parallel}$ is accurate to $\pm$ 10% (except for $\langle 111 \rangle$ stress, $\pm$ 30%). The height of the lines above and below the horizontal line represent the intensity polarized $\perp$ and $\parallel$ to the stress, respectively.
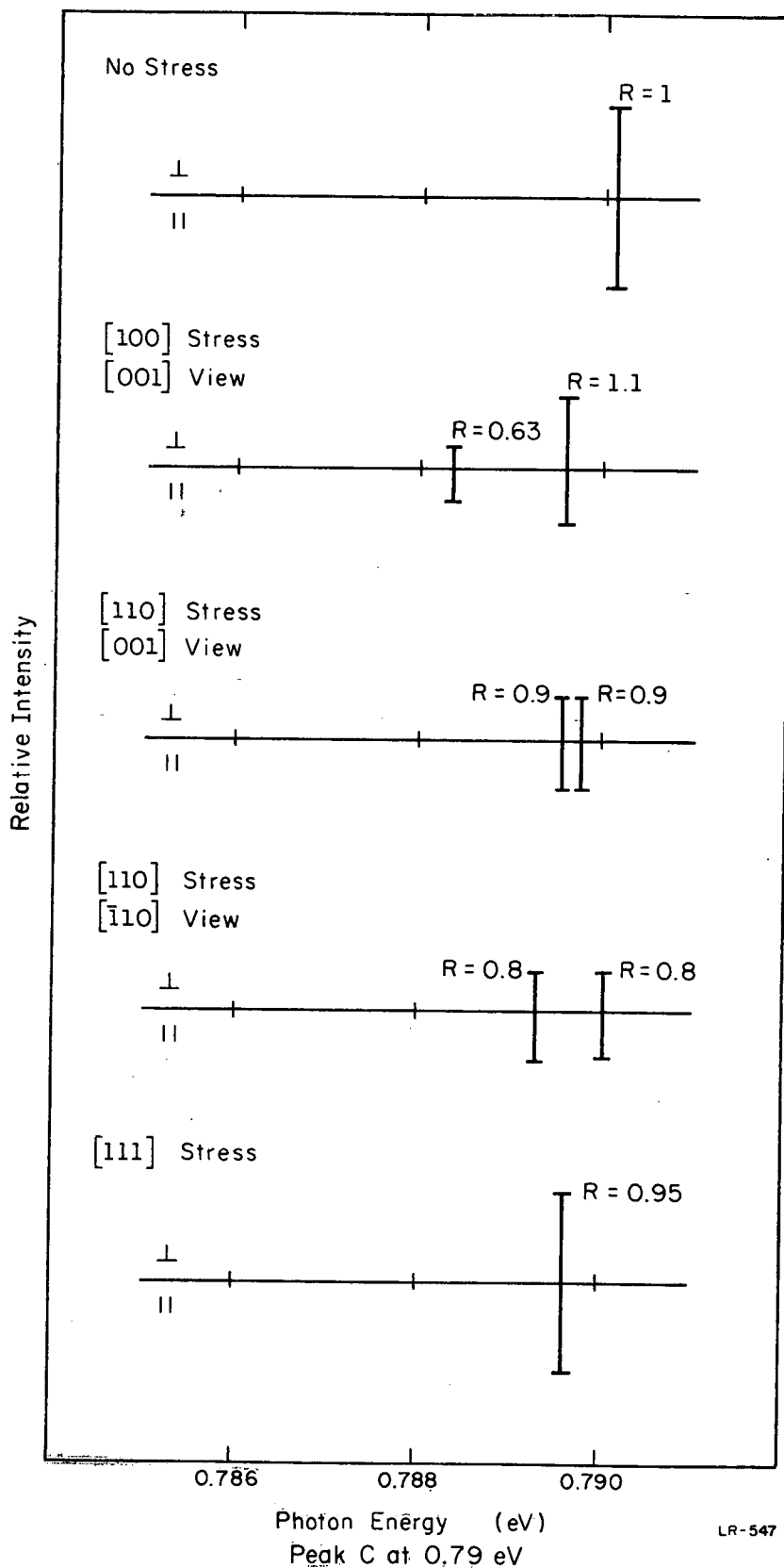
Figure 32.   Representation of the stress splittings and polarization of the
0.79 eV peak with $R = I_\perp/I_{||}$.   The height of the lines above and
below the horizontal line represent the intensity polarized $\perp$
and $||$ to the stress respectively.
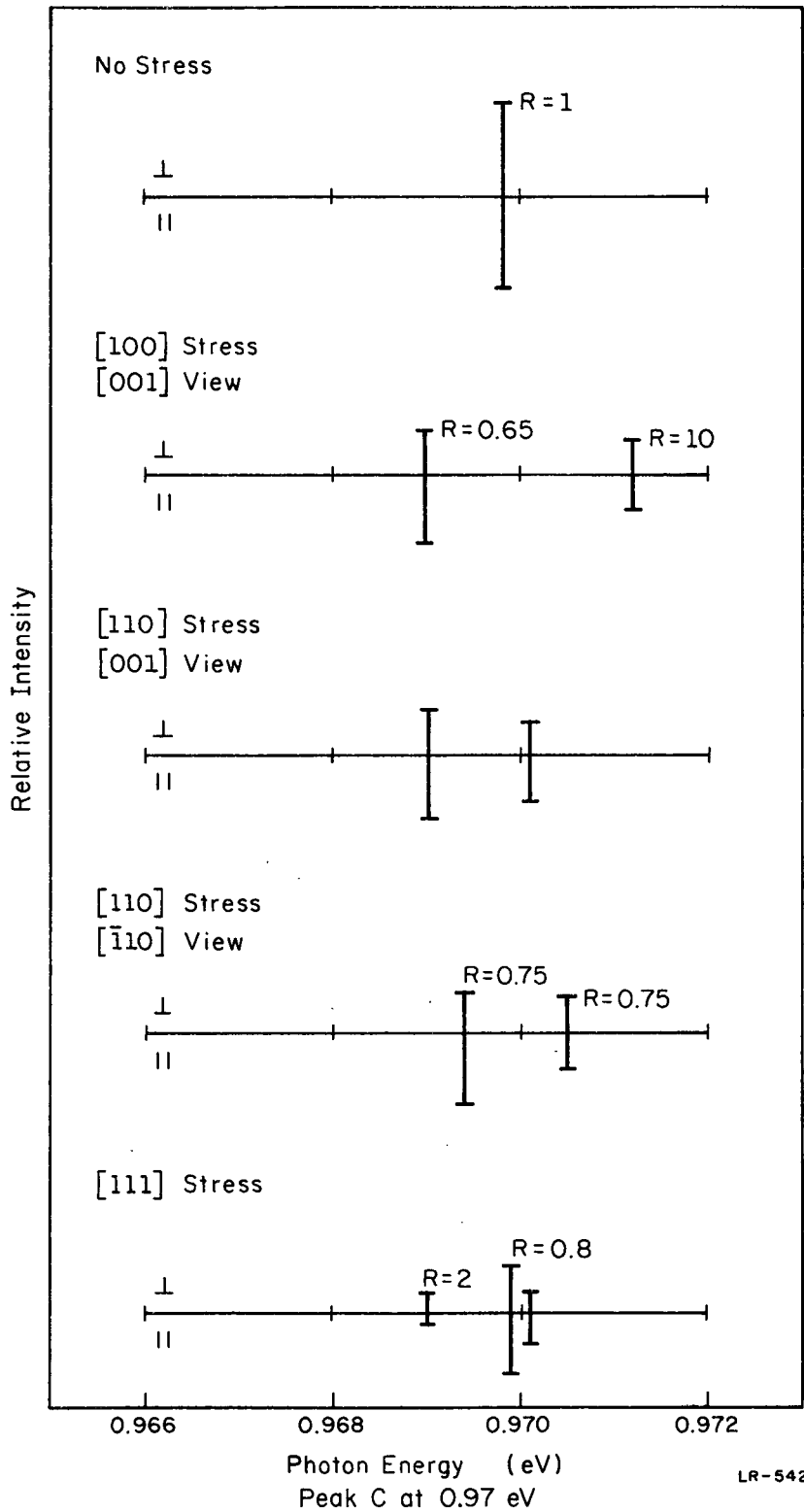
Figure 33.   Representation of the stress splittings and polarizations of the 0.97 eV peak with $R = I_\perp/I_{||}$.

IV. Analysis and Conclusions

4.1 Nature of the Transitions

The temperature dependence of the halfwidth of line 0.79 eV given in Fig. 6 is typical also of lines G and Q. If a free carrier were involved in these transitions the line widths would be thermally broadened. The halfwidth of a Boltzmann distribution is approximately 2 kT. Such a broadening can be seen, for example, in the width of the free exciton band-to-band luminescence in unirradiated silicon. It is clear from the data that the halfwidths of peaks C, G, and Q are much smaller than kT. In addition, the halfwidths do not depend linearly upon temperature. This indicate that a transition between a bound state and one of the bands is unlikely. We conclude, therefore, that the transition in each case is between two bound states.

There are several types of transitions involving bound states in silicon which have been investigated experimentally and theoretically. The various possibilities have been discussed in detail in References 2 and 3. Of the possible bound transitions, the most likely process involves a neutral defect which has a trapping level for one type of carrier. The opposite carrier is then bound by Coulombic attraction, and the radiation process occurs when the bound electron and hole recombine.

The characteristic form of the luminescence with a sharp zero-phonon line and lower energy phonon assisted peaks is due to transitions in the crystal which are analogous to the Mössbauer effect for nuclear transitions. In the Mössbauer effect an excited nucleus decays by

giving off a gamma-ray. If the recoil momentum of the nucleus is smaller than its zero point momentum, there will be a finite probability of leaving the nucleus in its ground state. The transition results in a narrow zero-phonon line. In the case of an optical transition at a crystal defect, the surrounding atoms have different equilibrium positions depending on whether the electron is in an excited state or the ground state. If the recoil momentum of the surrounding lattice atoms is smaller than the ground state momentum, there will be a finite probability for a zero-phonon transition. The lower energy bands then involve the transitions taking place along with the emission of phonons.

4.2 Identification of Peaks G(0.97eV) and C(0.79eV)

4.2.1 Stress Measurement

The narrow half-widths of the zero-phonon lines make it possible to measure shifts and splitting produced by stress (Fig. 30). The splittings depend upon the defect symmetry, the electronic wave functions, and any defect reorientation or electron redistribution which takes place under the stress.

Group theory helps make the analysis more specific. For each defect symmetry class group theory indicates what the degeneracies are and where the orbital dipole moments can be directed. For each symmetry class and type of transition, for example electric dipole, magnetic dipole etc., the splittings and the polarizations can be calculated. Calculations of this type have been done for defects in cubic crystals by A. A. Kaplyanskii[5] and Hughes and Runciman.[6] The results of the stress

data on the luminescence peaks have been discussed in detail in Reference

2. For the C peak at 0.79 eV the pattern suggests a ⟨100⟩ defect and

the pattern corresponds to that expected from a ⟨100⟩ tetragonal E to E,

doublet to doublet, electric dipole transition. The pattern expected

from a tetragonal ⟨100⟩ singlet to singlet transition is similar to the

observed pattern, except that the close doublets are single lines. The

fit between the 0.79 eV C peak and the tetragonal patterns is not good

enough to make a positive identification. The single line observed

under [111] stress is characteristic of a defect oriented along a

⟨100⟩ axis, but some of the polarizations and smaller splittings do not

compare. The splitting of the G peak at 0.97 eV is consistent with the

pattern for a trigonal [111] A→E, singlet to doublet, transition.

4.2.2 Correlation of Peak G(0.97 eV) with the Divacancy

Figure 34 is a composite of the isochronal annealing data for

peak G. The figure shows that peak G begins to anneal at $225°C$ and

vanishes in the temperature range 275 to $325°C$. Annealing occurs at a

slightly higher temperature in float zone silicon than in pulled silicon.

Furthermore, the data for p-type float zone silicon suggest a two-stage

annealing process, whereas the data for pulled silicon suggest a single-

stage annealing process.

All of these observations are in agreement with the annealing

behavior of the divacancy. The most extensive data on divacancy annealing

has been obtained from a study of the 1.8 μ optical absorption band.[7, 10]

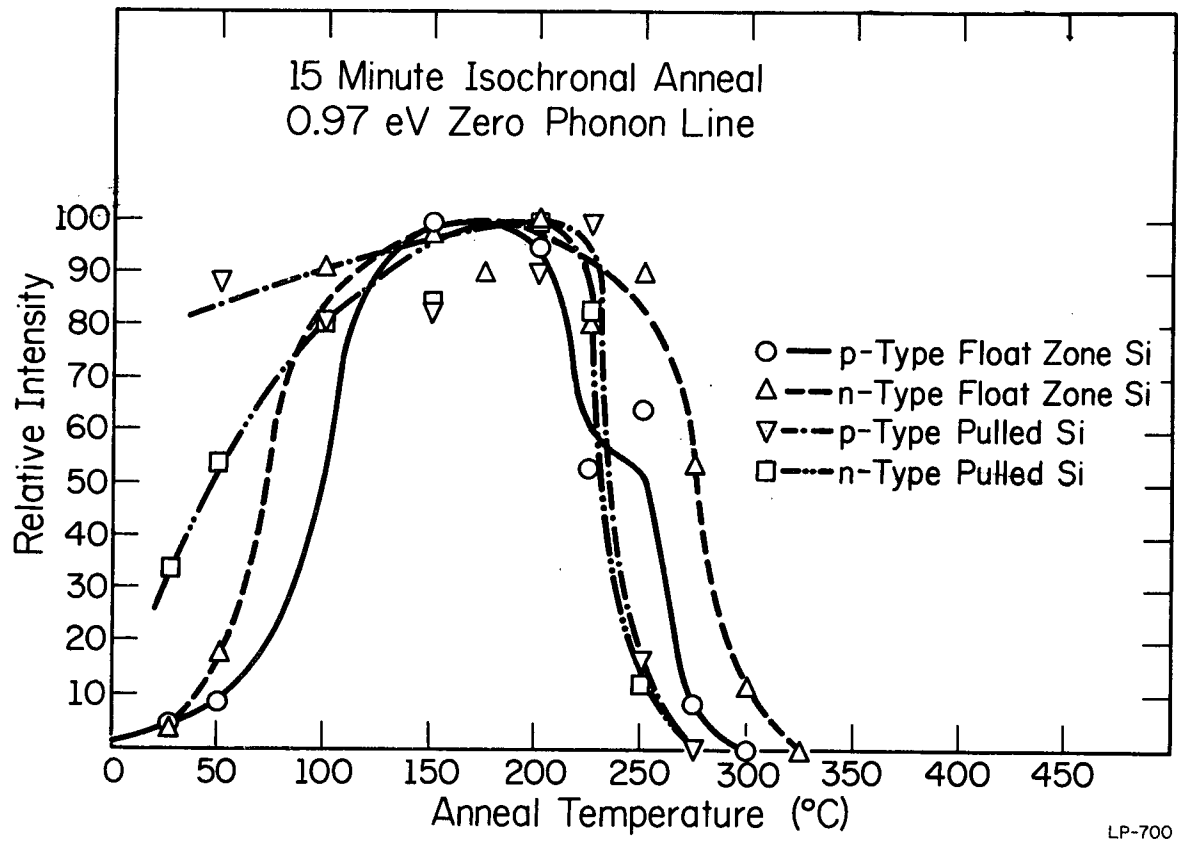As in the luminescence data, the divacancy absorption vanished in the

Figure 34. A composite display of the isochronal annealing data for zero-phonon peak G (0.970 eV). The data are taken from Figs. 10, 13, 17, and 22).

neighborhood of 275 to 325°C. Divacancy annealing occurs at a slightly

higher temperature in float zone silicon than in pulled silicon; furthermore,

the annealing in float zone silicon is a two-stage process, in contrast to

the single stage observed in pulled materials. Exact agreement of the

luminescence data with the absorption data cannot be expected because the

techniques have different detection thresholds and different annealing

schedules were performed.

Corelli[7] observed that two-stage divacancy annealing in float zone

silicon was enhanced by an increase in dopant impurity concentration, and he

suggested that the dissociation of a defect involving dopant impurities could

influence the annealing of the divacancy. Corelli suggested that the anneal-

ing properties of the E- and A-centers may contribute to several divacancy

annealing properties. The E-center anneals near 150°C[8] and is the dominant

center produced by irradiation in phosphorus-doped float zone silicon, whereas

the A-center anneals near 350°C and is the dominant center in phosphorus-doped

pulled silicon. The annealing of the E-center and the accompanying release

of vacancies could be responsible for two-stage divacancy annealing, whereas

the low E-center production in pulled material and stability of the A-center

could account for single-stage divacancy annealing in pulled silicon.

Several other properties of zero-phonon peak G are in good agree-

ment with the properties of the divacancy. Isothermal annealing measurements

of peak G in pulled silicon show that the activation energy is ~1.3 eV (Fig. 18).

This result is in agreement with EPR[9] and optical absorption[10] measurements,

which show the divacancy activation energy to be ~1.30 eV and ~1.25 eV, respec-

tively. The stress splittings of peak G best fit the trigonal ⟨111⟩ axial sym-

metry of the vacancies comprising the divacancy comples. Peak G is observed

in both pulled and float zone silicon, in agreement with the results of optical absorption[10,11] and EPR[9] studies of the divacancy.

The doping-impurity independence of the energy of peak G is important. This evidence is used, with other arguments, to eliminate from consideration those interstitial impurity defects which have annealing properties nearly identical to zero-phonon peak G. More generally, this impurity independence can be used to eliminate from consideration all centers involving dopant impurities.

Identification of peak G with the A-center is unlikely. The A-center is an oxygen-vacancy pair and may be visualized as a nearly sub-stitutional oxygen with two tetragonal bonds[12] in a plane along a ⟨110⟩ axis. These bonds and the long bond in a perpendicular plane between the nearest silicon atoms give the defect ⟨110⟩ axial symmetry. As mentioned previously, the stress splittings of peak G best fit the trigonal ⟨111⟩ symmetry class. Also, several features of the annealing data indicate that the A-center is inconsistent with the properties of peak G.[3] Finally, direct[13] and indirect[14] measurements of the A-center population agree that the A-center production rate is higher in pulled material than in float zone material. This fact is not inconsistent with the data for peak G shown in Fig. 34. It should be pointed out, however, that the maximum intensity of peak G measured during the anneal sequence is slightly higher in float zone silicon than in pulled silicon. It is difficult to under-stand how the A-center population in float zone silicon, which is of the order of the detection threshold of microscopic probes, could be influenced by annealing such that float zone silicon would have a greater A-center

population than pulled silicon.

Thus, close examination shows that the A-center symmetry, annealing, and population properties do not agree with the respective properties of peak G. Only the energy level shows close agreement and that appears to be coincidental.

The mass of the evidence supports the identification of the recombination center responsible for peak G (0.97 eV) with the divacancy. The annealing properties and symmetry are in good agreement with this association. The impurity independence of peak G rules out identification with dopant impurities, and impurity complexes involving oxygen, carbon, or germanium also seem unlikely. There are, however, several questions which may be raised regarding the association of peak G with the divacancy.

The defect energy level associated with peak G can be no deeper than 0.19 eV from a band edge. None of the energy levels reported for the divacancy satisfy this requirement.[15] The shallowest level reported is at E_v + 0.25 eV. A review of the literature on the divacancy energy levels shows that this problem is not as serious as it first appears. Divacancy levels obtained from EPR studies were reported at E_c - 0.40 eV, E_c - 0.55 eV, and E_v + 0.25 eV.[9,16,17] Photoconductivity levels at E_c - 0.39 eV and E_c - 0.54 eV were also associated with the divacancy;[18] these levels are in good agreement with the EPR levels. However, the literature does not give a consistent value for the energy of the shallow levels. Until these ambiguities are resolved by a consistent interpretation, one can only state that a shallow divacancy level exists. This is consistent with the data for peak G.

Although not explicitly shown in the data because normalization was based on maximum intensity, the absolute intensity of peak G following room temperature anneal was ~5 to 15 times greater in pulled silicon than in float zone silicon, consistent with the difference in divacancy production rates for these materials. The increase in the intensity of peak G during annealing in float zone silicon and the relative lack of increase in pulled silicon is consistent with the fact that divacancies are readily formed by vacancy-vacancy trapping in float zone silicon, whereas this mechanism is severely restricted in pulled silicon.

4.2.3 Correlation of Peak C (0.790 eV) with the K-Center

The annealing properties of peak C are unusual because of the wide temperature range over which the peak was observed. A well-known center identified in EPR studies which has similar annealing properties is the K-center.[19,20] A comparison of the annealing data for peak C and the K-center is shown in Fig. 35. The K-center annealing is shown only for p-type pulled silicon because the charge state in which the EPR spectrum can be observed is found only in this material. The annealing curve of the peak C in p-type pulled silicon is in excellent agreement with the K-center annealing. The annealing curve of peak C in n-type silicon does not compare as well with the K-center annealing but the essential features of observation over the same wide temperature range and persistence to 500°C continue to suggest correlation with the K-center. Goldstein[20] suggested that the reverse annealing of the K-center observed at 250°C is due to the formation of K-centers during divacancy annealing.
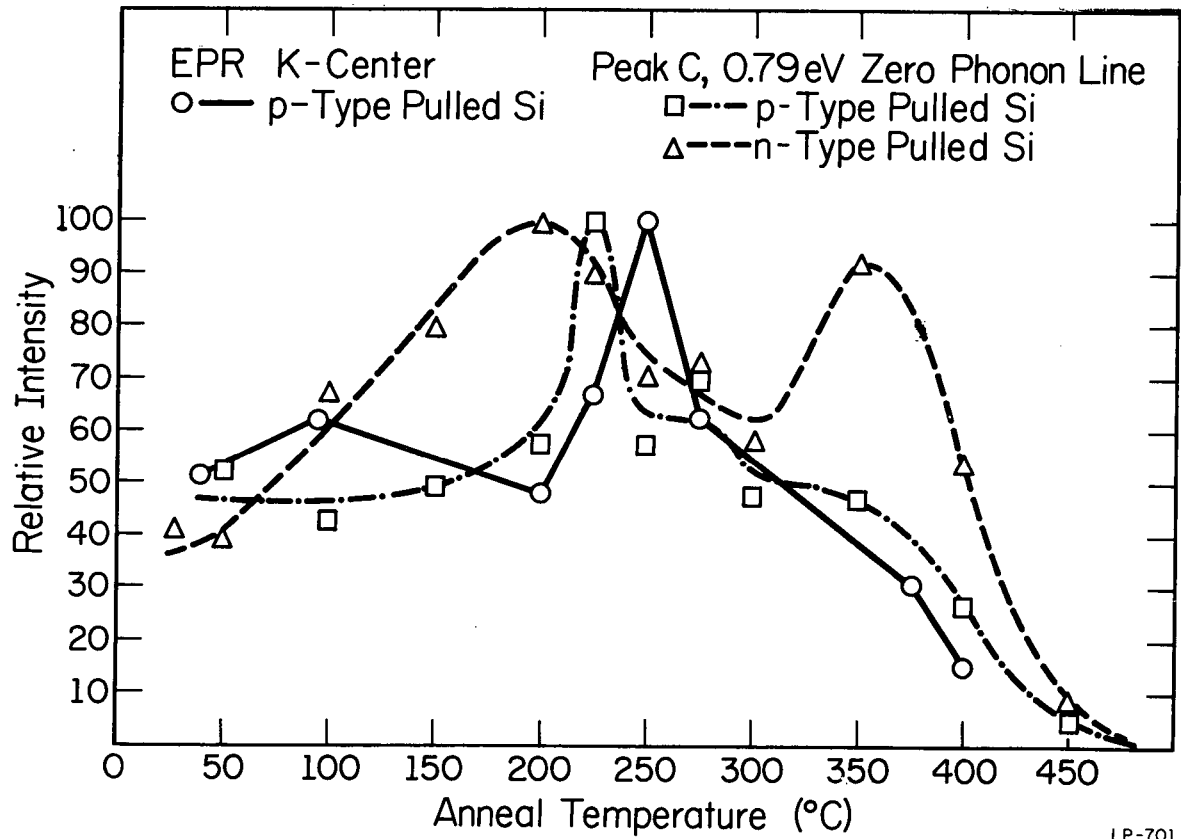
Figure 35. A comparison of the isochronal annealing of zero-phonon peak C (0.790 eV) and the K-center. The annealing data for peak C are taken from Figs. 17 and 22. The K-center data are taken from the EPR measurements of Goldstein et al.[20]

A similar reverse annealing for peak C at 350°C in n-type pulled silicon could be due to A-center annealing. It should be pointed out, however, that optical absorption studies have shown no appreciable difference between the A-center concentration in p- and n-type pulled silicon,[4,21] so that no explanation may be given for the lack of reverse annealing of peak C in p-type pulled silicon.

Other properties of the center responsible for peak C are in agreement with the K-center. Both centers are observed in pulled silicon but not in float zone silicon, the K-center being the dominant paramagnetic center in p-type pulled silicon.[19] The energy level of the center associated with peak C can be no deeper than 0.37 eV from a band edge. The energy level associated with the K-center, at E_v + 0.3 eV, is in good agreement.

The only major point of disagreement concerns the symmetry. We have shown that the stress splittings of peak C are best described by the symmetry class tetragonal $\langle 100 \rangle$, whereas Goldstein[20] observed a K-center symmetry axis of $\langle 221 \rangle$. This contradiction has not been resolved.

4.3 Luminescence in the Energy Region 0.98 to 1.16 eV - Pretail

A broad band of irradiation-dependent luminescence was observed between 0.98 and 1.16 eV in all samples following a twenty-minute room temperature anneal. The pretail is not a part of the spectrum shown in Fig. 5 associated with peak G. It is generally structureless; that is, there are no zero-phonon peaks or phonon replication. The intensity of the pretail is greater in float zone silicon than in pulled silicon; it

is also greater in p-type silicon than in n-type silicon. It follows that the pretail is most intense in p-type float zone silicon and least intense in n-type pulled silicon. In pulled silicon the pretail anneals out at a lower temperature ($<100^{\circ}$C) than it does in float zone silicon ($<200^{\circ}$C).

A model for the process which may be responsible for this luminescence has been presented.[3] The model suggests that carbon is involved in the defect responsible for this luminescence. This model is speculative and awaits further investigation. Therefore, it will not be explored here.

4.4   The High-Temperature Anneal Spectra

The luminescence spectrum associated with zero-phonon peak G at 0.97 eV was shown to vanish following anneal near 300°C. It was also shown that a number of different spectra, whose profiles were similar but not identical to the 0.97 eV spectrum, grew in upon further annealing in the temperature range 300 to 600°C. Each of these spectra was characterized by a sharp zero-phonon peak which grew in and annealed out independent of the other spectra. Thus, zero-phonon peaks F, H, J, K, L, and M seen following high-temperature anneal may each be associated with a unique defect.

It is of interest to compare the annealing data from the present work with that from a previous Russian investigation.[22,23] The annealing data reported by the Russian authors are shown in Fig. 36. The Russian measurements were taken at liquid nitrogen temperature. At this temperature the silicon band-gap is $\sim$1.162 eV as compared to 1.165 eV at liquid
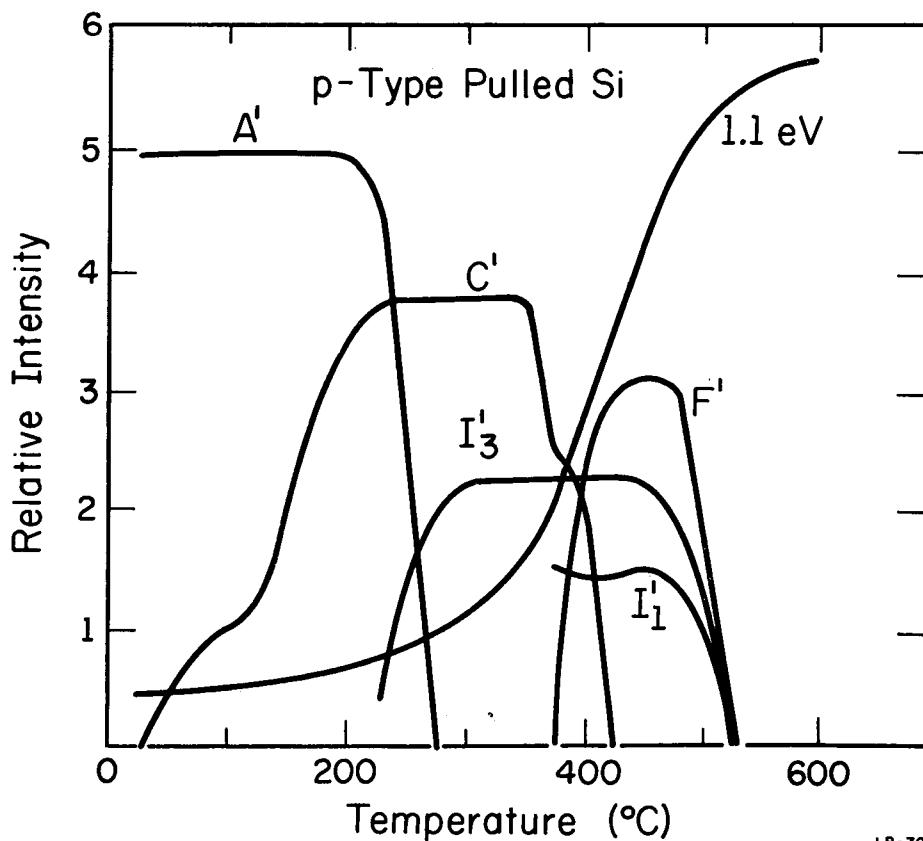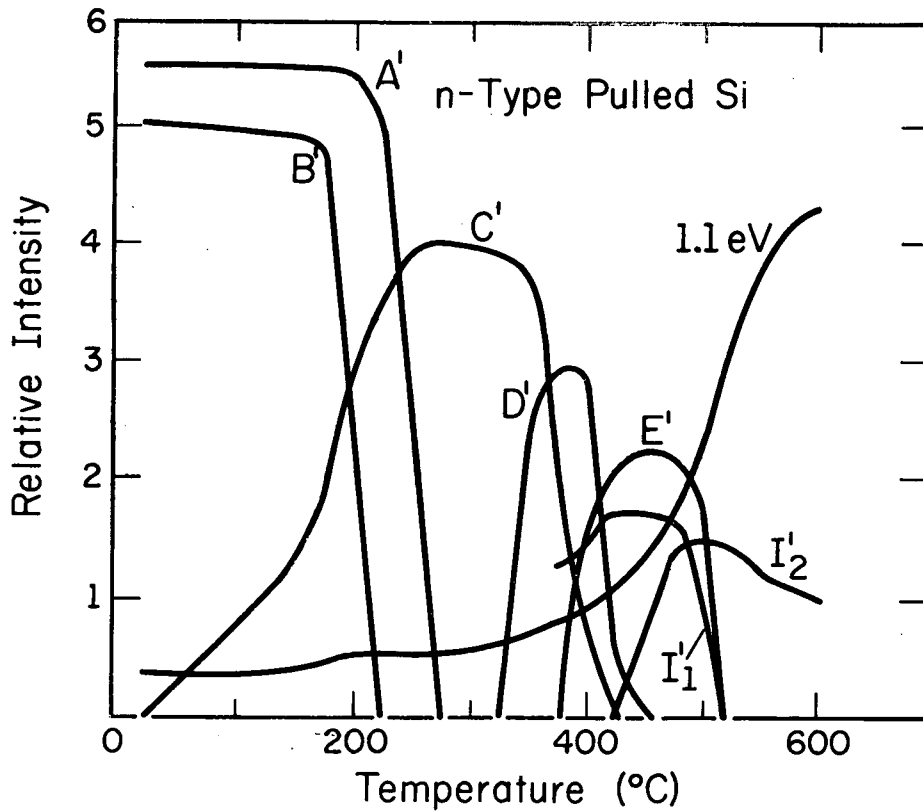
Figure 36. Isochronal annealing (twenty-minute anneals at 25° intervals) of the various zero-phonon peaks observed by Russian authors. The phosphorus concentration in n-type silicon was $5 \cdot 10^{15}$ atoms/cm^3 whereas the boron concentration in p-type silicon was $1 \cdot 10^{15}$ atoms/cm^3. The samples were irradiated by Co^{60} gamma-rays to a fluence of $5 \cdot 10^{17}$ / cm^2 (after Yukhnevich, Tkachev, and Bortnik[23]).

helium temperature. Therefore, one would expect the energy of the zero-phonon peaks taken at $77^{\circ}K$ to be shifted to lower energy with respect to the data taken at liquid helium temperatures by $\sim$3 meV. The comparisons which may be made between the Russian data and that from the present investigation follow.

The energy of peak A'(0.967 eV) in the Russian data compares well with peak G (0.970 eV). The Russian annealing data for this peak is also in excellent agreement with the annealing of peak G in pulled material.

Peak C' (0.790 eV) in the Russian data is the equivalent of peak C (0.790 eV) seen in this investigation. The Russians observed this peak to grow in by a factor $\sim$10 between room temperature and $200^{\circ}C$ in contrast to the limited growth observed for peak C in the present investigation. The lack of any reverse annealing stages and a lower annealing temperature at which peak C' vanishes are also in contrast with the results of the present investigation.

Peaks D'(0.945 eV) and E'(0.922 eV), observed by the Russians in n-type pulled silicon, correspond to peaks F (0.950 eV) and K (0.925 eV) observed in the present investigation. The annealing of peaks D' and E' correspond to that of peaks F and K (Figs. 17 and 22), except that the maximum for peak D' occurs $\sim25^{\circ}C$ lower than the maximum for peak F. The Russian authors observed these peaks only in n-type pulled silicon and attributed them to centers dependent on phosphorus for their formation. An important result of the present investigation is that these peaks appear in both n- and p-type pulled silicon; therefore, the corresponding defects are not dependent on doping impurities but only on impurities such as

oxygen, carbon, and perhaps germanium, which are present in larger concentrations in pulled silicon than in float zone silicon.

Weak, broad peaks, designated as I_1', I_2', and I_3' were also observed by the Russian authors. These peaks were not observed in the present investigation. It seems likely, however, that zero-phonon peak L (0.767 eV), which did appear in the present investigation at the same energy as I_1' may have been misinterpreted as a broad band by the Russians due to temperature broadening at their higher temperature of measurement.

It is known that heat treatment of pulled silicon at temperatures $\sim 500^{\circ}C$ produces oxygen aggregates which act as donors.[24] Luminescence peaks F, K, L, and M cannot be related to such aggregates, since these peaks have been shown to be irradiation dependent. No such peaks appear after heat treatment of unirradiated pulled silicon.

A number of irradiation-induced optical absorption bands which have annealing properties similar to peaks F, K, and L, have been observed in pulled silicon. At the present time only speculative correlation can be made between the luminescence peaks and these absorption bands, because little is known about the luminescence peaks and absorption bands other than their annealing properties and that they involve residual impurities found in pulled silicon.[3] Since correlations of these lines with known defects is speculative, they will not be discussed here.

4.5   Recombination Luminescence from Irradiated Lithium-Diffused Silicon

4.5.1   Float Zone Silicon

In this section we discuss the data involving lithium-doped material. Since the results for oxygen-rich (pulled) and oxygen-lean (float zone) material are quite different, we present these materials separately.

Peak Q, which dominates lithium-doped float zone material, is a zero-phonon line due to a bound-to-bound transition. Comments presented in relation to peaks C and G apply to this line.

The data presented in Chapter III show that lithium impurity has a large effect on the luminescence spectra from irradiated silicon. In lithium-diffused float zone silicon ($\geq 5 \cdot 10^{16}$ Li/cm^3) the luminescence spectrum associated with peak G is not present and is replaced by a spectrum (Fig. 23) from a new recombination center.

Lithium doping shifts the energy of the intrinsic free exciton recombination but does not quench the luminescence. Irradiation to a fluence of approximately 10^{16} e/cm^2 quenched the intrinsic luminescence in lithium-doped silicon, but produced no defect luminescence. The recombination centers formed must be of a nonradiative nature. Strong luminescence from the new spectrum was not observed until the fluence reached 10^{18} e/cm^2. This fluence is an order of magnitude greater than that needed to see luminescence of comparable intensity from peaks C and G in lithium-free pulled silicon. This suggests that the production of the new center is quite low, on the same order as the direct divacancy production rate in lithium-free float zone silicon. A second explanation for the high fluence might be that the luminescence efficiency is low for the center associated with peak Q. It will not be possible to distinguish between intensity

differences due to differences in defect introduction rate and luminescence efficiency until the luminescent centers are positively identified and their production rates measured by some other technique.

The impurity concentrations present in the lithium-diffused float zone silicon samples used in this investigation were estimated to be:: boron or phosphorus, $\sim 5 \cdot 10^{14}$ atoms/cm^3; oxygen, $\leq 10^{16}$ atoms/cm^3; carbon, $\leq 10^{16}$ atoms/cm^3; and lithium, $\geq 5 \cdot 10^{16}$ atoms/cm^3. Boron and phosphorus are not involved in the defect responsible for peak Q in this material, since the luminescence is independent of these impurities. The defect does not involve oxygen or carbon, since these trace impurities appear with greater concentrations in pulled silicon than in float zone silicon. If the defect responsible for peak Q involved oxygen or carbon one would expect the luminescence intensity to be much stronger in pulled than in float zone silicon. In fact, the opposite is observed, indicating that whereas oxygen and carbon may be involved in processes which may compete with the defect associated with peak Q, they do not participate directly in the formation of this defect. The data suggest, therefore, that only lithium and intrinsic defects are involved in the defect responsible for peak Q.

The disappearance of peak G and the appearance of lithium-dependent peak Q can be explained by three possible mechanisms. First, lithium prevents the formation of the defect associated with peak G and a new radiative center involving lithium is created. Second, the defect associated with peak G is formed and lithium is readily trapped at this center to form a new radiative center. Third, the defect associated with peak G is formed and lithium is trapped to form a nonradiative center; independently,

a new radiative center dependent on the presence of lithium is created.
A fourth possibility, that the defect responsible for peak Q is always
present in irradiated silicon and is only observed when peak G is quenched
is highly unlikely since peak Q is not observed in lithium-free float
zone silicon annealed between 300 and 400°C. (Peak G has annealed out
in this temperature range, peak Q should not have.) The following dis-
cussion will show that the second mechanism is most likely.

It is well-known that impurity-vacancy defects such as the A-
and E-centers possess negative charge states in n-type silicon. Due to
their negative charge these and other centers are effective hole traps,
and their presence degrades the minority carrier lifetime. Lithium in
silicon is an interstitial donor. The Li$^+$ ion is mobile at room tempera-
ture[25] and should be easily trapped by negatively charged defects.
Wysocki[26] has presented strong evidence that the negatively charged defects
in lithium-diffused silicon are neutralized by trapping a Li$^+$ ion. As an
example, the mechanism for E-center neutralization was suggested by Wysocki
to be

$$Li^+ + (P-V)^- = Li-(P-V).$$
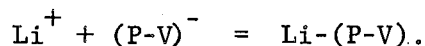
The hole capture cross section for the resulting neutral center is expected
to be two or three orders of magnitude smaller than that for the negative
center. According to this model, the minority carrier lifetime would not
be strongly affected by the resulting neutral defects, whereas the carrier
concentration would remain degraded.

It has also been shown that lithium forms recombination centers
with silicon vacancies and/or silicon interstitials.[26] In n-type material

the vacancy removes one electron from the conduction band and assumes the negative charge state. A "stable" defect involving lithium could be formed that would serve as a hole trap. This defect is of the form:

$$Li^+ + V^- + e^- = (Li-V)^-.$$
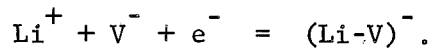
Goldstein[27] identified the only EPR spectrum in irradiated lithium-diffused float zone silicon with a Li-interstitial complex. Goldstein found that this center can account for only a small part of the majority carrier removal rate and he suggested that the remaining loss is due to the formation of the defect $(Li-V)^-$.

Wysocki proposed that the minority carrier lifetime degradation due to $(Li-V)^-$ could be removed through neutralization of the defect in the manner

$$Li^+ + (Li-V)^- = (Li-V)-Li.$$

Minority carrier lifetime recovery attributed to this mechanism was observed to take place at room temperature. The annealing process has an activation energy of ∼0.61 eV, a value very close to the activation energy for the diffusion of lithium in silicon, ∼0.66 eV. A similar value of the activation energy was found for the neutralization of the E-center. In the case of $(Li-V)^-$ neutralization Wysocki interpreted this to mean that lithium diffused to the defect rather than from it, since the dissociation of $(Li-V)^-$ would involve a small dissociation energy in addition to the activation energy for lithium migration.

The important points in terms of the present investigation are

that a lithium-vacancy complex forms and that annealing of this center occurs at room temperature. It is likely that this center and perhaps the lithium-silicon interstitial complex account for the nonradiative centers which quench the intrinsic luminescence in the present investigation. The spectrum associated with peak Q, which is stable to ~400°C, cannot be associated with these centers, however.

The above models of defects and formation mechanisms suggest three possible models for peak Q. The defect responsible may be lithium associated with the only intrinsic defect remaining, the divacancy; it may be the neutral center (LiV)-Li; or it may be a complex lithium precipitate. The first possibility best agrees with the data. The divacancy is produced directly by irradiation and would be formed at the direct production rate regardless of the lithium-vacancy-vacancy interaction which would inhibit divacancy creation through vacancy-vacancy trapping. In fact, the direct production rate for the divacancy in float zone silicon is consistent with the high fluence necessary to observe strong luminescence from peak A. In highly n-type silicon the divacancy has a doubly-negative charge state and should easily trap mobile Li^+ ions in a manner similar to the E-center neutralization

$$(V + V)^= + 2Li^+ = Li\text{-}(V + V)\text{-}Li$$
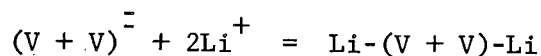
In the previous section arguments were presented for identifying the recombination center responsible for zero-phonon peak G with the divacancy. This assignment is consistent with the present model for peak Q, in that the spectrum associated with peak G is not observed in lithium-diffused

float zone silicon.

The lithium-dependent recombination center found in this study fits into the theory of damage processes in heavily lithium-doped float zone silicon as follows. Irradiation produces vacancies, interstitials, and divacancies as primary defects; these defects trap electrons and assume negative charge states, thereby reducing the carrier concentration. In the negative charge state the defects are hole traps and therefore degrade the the minority carrier lifetime. If lithium is present the damage center may be neutralized by trapping Li^+ ions, thereby reducing the hole capture cross section. When this occurs the center is no longer an effective hole trap, and recovery of the minority carrier lifetime occurs. The defect associated with peak Q is probably one of the end products of recovery, most likely a lithium-modified divacancy. Unfortunately, it is impossible to make a direct correlation between the growth of peak Q and the recovery of room temperature carrier lifetime, since the detection thresholds for the two measurements differ by several orders of magnitude.

This speculative model is in agreement with the conclusions of Young et al.[28] These authors attributed the lithium-dependent optical absorption bands at 1.4 and 1.7 μ to electronic transitions of a lithium-modified divacancy.

Comparison of the splitting data for peak Q (1.045 eV), with the results of group theory shows that the data best fit the trigonal $\langle 111 \rangle$ orientational symmetry class. The data imply that no electronic degeneracies are lifted by the stress. The orientational symmetry is

consistent with the model previously suggested for the defect associated with peak Q. The vacancies forming the divacancy lie along a $\langle 111 \rangle$ axis. Therefore, a lithium ion trapped in the nearest interstitial position along the divacancy axis would produce a defect with the observed symmetry. A divacancy with two substitutional lithium atoms (the divacancy may be doubly negative in n-type material) would also agree with the observed symmetry.

4.5.2 Pulled Silicon

Lithium impurity has a less pronounced effect on the luminescence spectra from pulled silicon than is the case for float zone silicon. Zero-phonon peaks C and G were observed, but a fluence of 10^{18} e/cm^2 was required to produce reasonable intensity. Peak C was much weaker than peak G in lithium-diffused pulled silicon, whereas the peak intensities were approximately equal in lithium-free silicon. In addition, the spectrum associated with zero-phonon peak Q was observed at low intensity. Several new peaks were observed following high-temperature anneal. The data suggest that lithium does not readily associate with luminescent centers in pulled silicon and that oxygen does not readily associate with primary defects to form oxygen-dependent centers.

The present understanding of the behavior of lithium in pulled silicon is based on the existence of the LiO$^+$ donor. Pell[29] showed that the lithium in pulled silicon associates with oxygen to form the interstitial donor LiO$^+$, provided the concentration of lithium does not exceed the concentration of oxygen. Such was the case for the lithium concentration

in the pulled silicon used in this investigation. It is believed that the LiO^+ ion interacts with vacancies[30] and interstitials[27] to form defects in a manner similar to the Li^+ ion in float zone silicon, that is,

$$LiO^+ + V^- + e^- = (LiO-V)^-$$
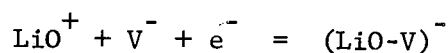
Unlike Li^+ the ion LiO^+ is not mobile at room temperature because the lithium is tied to the immobile oxygen interstitial. Damage recovery must involve the Li^+ ion which is always present to some extent. Defects such as the E- or A-centers will anneal according to the equation described earlier. The defect $(LiO-V)^-$ will anneal in a similar manner,

$$(LiO-V)^- + Li^+ = (LiO-V)-Li.$$
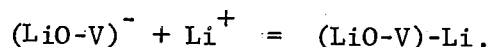
The activation energy for this process has been found to be $\sim$0.60 eV,[31,32] again suggesting that lithium is moving about and is responsible for the annealing. Recovery requires elevated temperatures ($\sim$150°C)[33] or very long periods of time at room temperature.[32] This lack of rapid low temperature annealing is due to the fact that the diffusion constant for lithium in silicon is replaced by an effective diffusion constant because of the influence of Li^+ coupling and decoupling with interstitial oxygen.[34] That is, the formation of LiO^+ is an equilibrium relationship,

$$Li^+ + 0 \rightleftharpoons LiO^+.$$

The effective diffusion is given by

$$D_{eff} = D_o/(1 + \frac{[0]}{C}).$$

In this expression D_o is the diffusion constant of lithium ions in the absence of oxygen, $[0]$ is the concentration of oxygen, and C is the reaction constant for the formation of the LiO^+ ion. At room temperature D_{eff} for silicon containing oxygen in concentrations of $\sim 10^{17}$ atoms/cm^3 is two orders of magnitude smaller than D_o.

A qualitiative explanation for the luminescence spectra from lithium-doped pulled silicon can now be presented. Prior to irradiation, most of the lithium is tied up with oxygen in the form of LiO^+ donors so that the concentrations of mobile lithium and interstitial oxygen available to associate with vacancies or to form higher complexes are greatly reduced. Irradiation produces vacancies, interstitials and divacancies. Migrating vacancies are trapped by LiO^+ to form $(LiO-V)^-$ defects. A small equilibrium concentration of Li^+ is available to trap vacancies and to be trapped by divacancies. In this manner a small number of lithium-modified divacancies are produced. In addition, the concentration of oxygen-dependent centers such as the K-center will be smaller than that for lithium-free silicon, since much of the oxygen is tied up as LiO^+ or $(LiO-V)^-$. All of these suggestions are in agreement with the luminescence data.

4.5.3 Summary

The results of the present study of irradiated lithium-doped silicon help to explain the damage recovery observed in silicon devices containing lithium. It was shown in this investigation that luminescent

centers usually seen in irradiated oxygen-lean silicon are not observed when sufficient lithium is present, and that a lithium-dependent center is formed whose trapping level is too shallow to have an effect on the room temperature minority carrier lifetime. Previous studies using EPR and electrical techniques have indicated the nature of the interaction between lithium and the silicon vacancy and interstitial. The present investigation suggests that the interaction between lithium and the remaining primary defect, the divacancy, is of a similar nature, in that lithium migrates to and neutralizes negatively charged centers, thereby reducing the hole capture cross section several orders of magnitude and effecting recovery of the minority carrier lifetime.

V. SUMMARY AND RECOMMENDATIONS

Recombination luminescence has been shown to be a powerful technique for studying defects induced in silicon by high-energy irradiation. The luminescence observed following irradiation has the characteristic form of a narrow zero-phonon peak with lower-energy phonon-assisted peaks. Significant progress toward identification of the defects responsible for luminescence has been made in this investigation. The results for lithium-free silicon are given first.

The luminescence associated with zero-phonon peak G (0.97 eV) is believed due to recombination involving the divacancy. The isochronal and isothermal annealing of this peak are in good agreement with divacancy annealing. The production rate, stress splittings, and impurity independence of the luminescence are also in agreement with the assignment of peak G to the divacancy.

The isochronal annealing of zero-phonon peak C (0.79 eV) is in good agreement with annealing of the K-center. The energy of the peak and the oxygen dependence of the luminescence are also consistent with this assignment.

A broad band of weak luminescence is observed between 0.98 eV and 1.16 eV following room temperature anneal. The intensity of this luminescence is greater in float zone silicon than in pulled silicon and greater in p- than in n-type silicon. A highly speculative model which attributes the luminescence to donor-acceptor pairs involving carbon is suggested.

A number of new spectra are observed following high-temperature anneal. Zero-phonon peaks F (0.950 eV), K (0.925 eV), and (0.767 eV) are observed in both n- and p-type pulled silicon. The defects responsible for these peaks are thought to be dependent on oxygen. Zero-phonon peak M (0.760 eV) is observed only in p-type pulled silicon and thus the defect responsible probably involves both boron and oxygen. The annealing of peaks F, K, and L suggests the association of these centers with centers observed and modeled in optical absorption work.

This investigation reports the first luminescence spectra from irradiated lithium-doped silicon. In float zone silicon peak G vanishes and a new spectrum associated with a strong zero-phonon peak at 1.045 eV (peak Q) is observed. Weak zero-phonon peaks N (0.990 eV), O (0.997 eV), P (1.013 eV), and R (1.048 eV) are also associated with this spectrum. The intensity of peaks Q and R are related by a Boltzmann factor in which the energy is given by the energy separation of the peaks. The new spectrum associated with peak Q is present following room temperature anneal and vanishes after annealing near 400°C. The transition mechanism involves recombination between two bound states. The stress splittings for peak Q best fit the trigonal $\langle 111 \rangle$ orientational symmetry class. No electronic degeneracies are lifted by the applied stress. It is likely that this spectrum involves recombination at a neutral center formed by a negative defect which has captured a Li^+ ion. The creation of this center is a likely cause for partial recovery of the room temperature minority carrier lifetime. The data are consistent with the assignment

of this spectrum to a lithium-modified divacancy.

The effects of lithium are less pronounced in pulled silicon. Zero-phonon peaks C and G are observed as in lithium-free silicon, but the production rates for these centers are reduced. Peak Q is present but at a low intensity, and a broad lithium-dependent band is found for energies below 0.83 eV. New zero-phonon peaks V (0.785 eV), W (0.878 eV), and X (1.001 eV) are observed following high-temperature anneal, as were zero-phonon peaks F, K, and L. The data are consistent with the known proper-ties of the LiO^+ ion. Formation of this defect restricts the migration of free lithium and reduces the concentration of interstitial oxygen. The ion associates with vacancies, thereby reducing the population of centers involving the vacancy.

Experiments which should be performed in later research in this area include the following:

1. Study of possible isotopic shifts in lithium dependent lines for material doped with Li^6.

2. Study of defects involving carbon by investigating carbon-doped silicon.

3. Irradiation of lithium doped float zone silicon at low temperatures. Upon annealing to room temperature, it should be possible to check the hypothesis that peak Q is formed when lithium diffuses to modify the divacancy center.

VI. REFERENCES

1. R. J. Spry and W. D. Compton, Phys. Rev. 175, 1010 (1968).
   R. J. Spry, Ph.D. Thesis, University of Illinois (1967).

2. C. E. Jones, Ph.D. Thesis, University of Illinois (1970).
   C. E. Jones and W. D. Compton, in 1970 Albany Conference on
   Radiation Damage in Semiconductors (to be published in
   Radiation Effects).

3. E. S. Johnson, Ph.D. Thesis, University of Illinois (1971).
   E. S. Johnson and W. D. Compton, in 1970 Albany Conference on
   Radiation Damage in Semiconductors (to be published in
   Radiation Effects).

4. J. R. Haynes, M. Lax, and W. F. Flood, J. Phys. Chem. Solids 8,
   392 (1959).

5. A. A. Kaplyanskii, Opt. i Spektroskopiya 7, 677 (1959) [English
   transl.: Opt. Spectry. 7, 406 (1959)] .
   A. A. Kaplyanskii, Opt. i Spektroskopiya 16, 602 (1964) [English
   trans.: Opt. Spectry. 16, 329 (1964)].

6. A. E. Hughes and W. A. Runciman, Proc. Phys. Soc. (London) 90,
   827 (1967).

7. J. C. Corelli, in Lattice Defects in Semiconductors, ed. by R.
   Hasiguti (University of Tokyo Press, Tokyo, 1968), pp. 265-
   281.

8. L. B. Valdes, Proc. IRE 42, 420 (1954).

9. G. D. Watkins and J. W. Corbett, Phys. Rev. 138, A543 (1965).

10. L. J. Cheng, J. C. Corelli, J. W. Corbett, and G. D. Watkins,
    Phys. Rev. 152, 761 (1966).

11. J. C. Corelli, G. Oehler, J. F. Becker, and K. J. Eisentraut,
    J. Appl. Phys. 36, 1787 (1965).

12. E. L. Elkin and G. D. Watkins, Phys. Rev. 174, 881 (1968).

13. J. W. Corbett, G. D. Watkins, R. M. Chrenko, R. S. McDonald,
    Phys. Rev. 121, 1015 (1961):

14. T. Tanaka and Y. Inuishi, J. Phys. Soc. Japan 19, 167 (1964).

15. H. J. Stein, in 1970 Albany Conference on Radiation Damage in
    Semiconductors (to be published in Radiation Effects).

16. G. D. Watkins, in Seventh International Conference on the Physics of Semiconductors, Vol. 3, Radiation Damage in Semiconductors, ed. P. Baruch (Academic Press, New York, 1964), pp. 97-113.

17. G. D. Watkins and J. W. Corbett, Disc. Faraday Soc., No. 31, 86 (1961).

18. A. H. Kalma and J. C. Corelli, Phys. Rev. 173, 734 (1968).

19. N. Almeleh and B. Goldstein, Phys. Rev. 149, 687 (1966).

20. B. Goldstein et al., "Analysis of Radiation Damage in Silicon Solar Cells and Annealing or Compensation of Damage by Impurities," C.F.S.T.I., N67-28927.

21. R. E. Whan, J. Appl. Phys. 37, 3378 (1966).

22. M. V. Bortnik, V. D. Tkachev, and A. V. Yukhnevich, Soviet Phys.-Semiconductors. English Transl. 1, 290 (1967).

23. A. V. Yukhnevich, V. D. Tkachev, and M. V. Bortnik, Soviet Phys.-Solid State. English Transl. 8, 2571 (1967).

24. W. Kaiser, H. L. Frisch, and H. Reiss, Phys. Rev. 112, 1546 (1958).

25. E. M. Pell, Phys. Rev. 119, 1014 (1960).

26. J. J. Wysocki, IEEE Trans. on Nucl. Sci. NS-14, No. 6, 103 (1967).

27. B. Goldstein, Phys. Rev. B 2, 4110 (1970).

28. R. C. Young, J. W. Westhead, and J. C. Corelli, J. Appl. Phys. 40, 271 (1969).

29. E. M. Pell, in Symposium on Solid State Physics and Telecommunications (Academic Press, New York, 1960), Vol. 1, p. 261.

30. G. J. Brucker, Phys. Rev. 183, 712 (1969).

31. J. A. Naber, in "Conference on the Physics and Application of Lithium Diffused Silicon," Goddard Space Flight Center, December, 1969, X-711-69-366, pp. 81-88.

32. P. H. Fang, Y. M. Liu, J. R. Carter, Jr., and R. G. Downing, Appl. Phys. Letters 12, 57 (1968).

33. P. H. Fang, in Lattice Defects in Semiconductors, ed. by R. Hasiguti (University of Tokyo Press, Tokyo, 1968), pp. 155-158.

34. E. M. Pell, Phys. Rev. 119, 1222 (1960).